CRC Report No. A-54-2

TRENDS IN WESTERN O_3 AND PM AND THEIR RELATIONSHIP TO FIRES AND METEOROLOGICAL VARIABLES

Phase 2
Final Report

September 2006

COORDINATING RESEARCH COUNCIL, INC.
3650 MANSELL ROAD·SUITE 140·ALPHARETTA, GA 30022

Trends in Western O_3 and PM and Their Relationship to Fires and Meteorological Variables

Prepared by:

Dr. Daniel Jaffe
Northwest Air Quality
7746 Ravenna Avenue NE
Seattle, WA 98115
nw_airquality@hotmail.com

Executive Summary

In September 2004, the CRC contracted with Dr. Daniel Jaffe for a project to examine the role that global sources, climate and biomass burning have on O_3 and particulate matter (PM) trends and variability in the western U.S. This report gives results from the second year of the project. The primary goals of this project are to understand inter-annual variations and long-term changes in O_3 and PM. The original objective of the study included an assessment of the role of inter-continental transport and it was determined that this factor could not readily be quantified. The influence of regional wildfires was observable and results of this assessment are presented in this report. The key findings are:

1) There is good evidence that O_3 at rural and remote sites in the western U.S. has increased over the past 2 decades. The mean increase, seen at 9 sites with data for at least 12 years is 0.3 ppbv/year. The O_3 trend appears to be present in all seasons;

2) Changes in temperature do not appear to be a significant cause for the trend in O_3 at these sites;

3) The relationship between monthly and seasonal area burned in the western U.S. with measured PM and O_3 concentrations was evaluated. Due to limitations of the fire database, using seasonal area burned gave the best results. For the western U.S., a significant relationship between area burned and seasonal mean O_3 was found. The slope of this relationship was 1.23×10^{-6} ppbv/acre burned. This means that for an average season (1.68 million acres), fires add 2.0 ppbv of O_3. For a large fire year (4-5 million acres), fires can add up 6 ppbv of O_3, averaged over the entire summer. Short term and local impacts can be much larger.

4) A statistically significant relationship between PM2.5 and area burned was also identified. Using the slope of this relationship, 3.7-4.9x10^{-7} ug/m^3/acre burned and the average area burned, we find that fires contribute between 0.6-0.8 ug/m^3 to PM2.5 across the western U.S. averaged over the summer. For a large fire year, fires can add 1.8-2.5 ug/m^3 of PM2.5, averaged over the entire summer. As with O_3, short term and local impacts can be much larger.

5) Between 1999-2003, the summer burned areas averaged 72% greater than the average for 1987-2003. While this cannot explain the O_3 trend we observed for all seasons, we believe this is a significant contributing factor for the summer trends.

Table of contents

1. Overview of O_3 data in the western U.S.

For this analysis, we are using data from 13 rural-remote sites in the western U.S. extending from Alaska to Colorado. Table 1.1 gives the location, as well as additional information for each site.

Table 1.1: Information on the 14 sites used in our analysis.

Location	Site type	Lat.(^{o}N)/Long.(^{o}W)/ elevation (meters)	Data record (mm/yy)
Lassen N.P., California	NPS	40.54/121.58/1756	10/87-8/04
Rocky Mtn. N.P., Colorado	NPS	40.28/105.55/2743	1/87-11/04
Yellowstone N.P., Wyoming	NPS	44.56/110.40/2400	4/87-8/04
Glacier N.P., Montana	NPS	48.51/114.00/976	4/89-10/04
Denali N.P., Alaska	NPS	63.73/148.96/661	7/87-11/04
Barrow, Alaska	NOAA/CMDL	71.32/156.60/11	3/73-12/03
Pinedale, Wyoming	CASTNET	42.93/109.79/2388	1/89-12/04
Gothic, Colorado	CASTNET	38.96/106.99/2926	7/89-12/04
Centennial, Wyoming	CASTNET	41.36/106.24/3178	7/89-12/04
Craters of the Moon N.M., Idaho	NPS	43.46/113.56/1815	10/92-12/04
Canyonlands N.P., Utah	NPS	38.46/109.82/1809	8/92-12/04
Cheeka Peak, Washington	University of Washington	48.3/124.6/480	Non-continuous since 1997
Trinidad Head, California	NOAA	41.05/124.17/107	Weekly ozonesonde launches since 1997
Boulder, Colorado	NOAA	39.95/105.25/1743	Weekly ozonesonde launches since 1985

These 14 sites are located predominantly in rural or remote regions of the west, and many are located in National Parks. We have used 11 of the surface O_3 monitoring sites to evaluate long-term trends. We will also examine trends using the Boulder ozonesonde data. Of the 11 surface sites used for trend analysis, 9 are in the continental U.S. and 2 sites are in Alaska. Figure 1.1 shows a map of the surface sites used for trend analysis, plus Cheeka Peak and Trinidad Head.

Figure 1.2 shows the seasonal pattern of O_3 at 7 of the sites in the western U.S. Two sites are clean background monitoring sites located immediately adjacent to the Pacific coast, however data from these sites goes back only to 1997. These two sites are Cheeka Peak (CP), Washington

and Trinidad Head (THD), California. The Cheeka Peak site is relatively low elevation at 0.5 km above sea level (asl). The Trinidad Head data are from balloon-borne ozonesondes measurements, averaged into two altitude ranges; 0-1.5 km and 1.5-3.5 km asl.

Figure 1.1: Map of the United States showing 11 sites used in O_3 trend analysis, plus two additional sites (Cheeka Peak, Washington and Trinidad Head, California).

Figure 1.2: Monthly mean O_3 mixing ratio at 7 sites in the western U.S. The sites are Trinidad Head (THD), Cheeka Peak (CPO), Yellowstone N.P., Rocky Mtn.N.P. (RMNP), Lassen N.P. and Centennial. The elevation of each site is given in the caption.

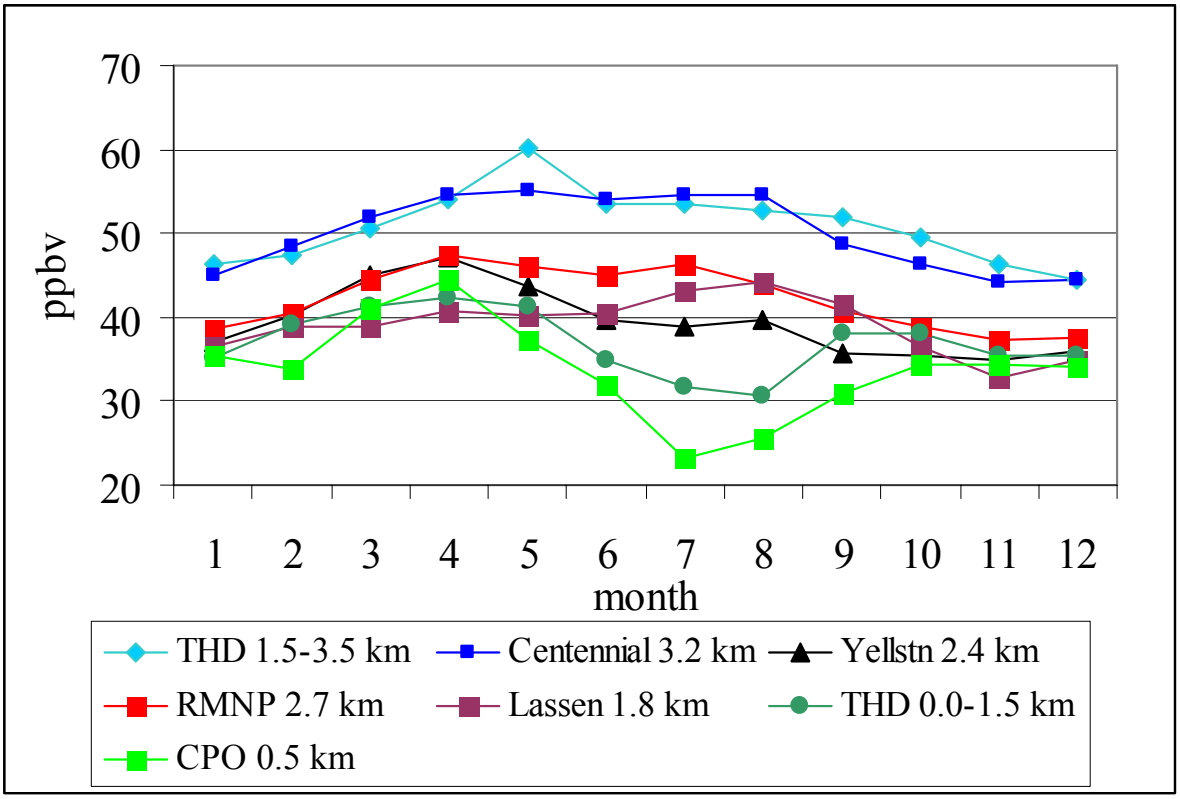

Examining Figure 1.2, we see that most sites show a spring maximum in O_3 mixing ratios. This peak is seen throughout the lower troposphere of the Northern Hemisphere, and reflects the influence from global background O_3. Some sites also show a summer peak, which is likely due to photochemical O_3 production from regional NOx and NMHC emissions. This is most apparent for Rocky Mtn N.P. and Lassen N.P., both of which are adjacent to major emission regions. The figure also shows the influence of altitude on O_3. Elevated sites generally have higher O_3 mixing ratios (e.g., Centennial and THD 1.5-3.5 km data). In fall through spring, concentrations are similar at most of the lower elevation sites. For example, the difference in monthly mean concentrations between CPO, THD (0-1.5 km) and the other sites is about 5 ppbv through most of the year; whereas in summer, this difference becomes much larger, 15-20 ppbv. This argues that the background influence is strongest in fall through spring, and reduced in summer as regional photochemical pollution becomes more important at the inland sites.

2. O_3 trend analysis for 11 sites in the western U.S.

The NPS reports annually on progress for meeting air quality goals in the National Parks. Their most recent analysis (March 2006) focuses on trends by Park in the 3-year average of the annual fourth highest daily maximum 8-hour concentration. (see http://www2.nature.nps.gov/air/who/npsPerfMeasures.cfm). While this metric is clearly important, it is not the only way to evaluate changes in O_3 concentrations for the western U.S. Our work focuses on changes in the mean O_3 concentrations by month and season, not just the highest O_3 days. Understanding changes in the mean O_3 concentration should give us insight into long-term changes for the days with highest O_3 concentration.

Ideally, we would like sites with long data records that have remained unchanged over many years. Unfortunately, perfect data records rarely exist. For many of these sites, a change in site location or inlet height was made in the mid 1990's. At Lassen, Rocky Mtn., Yellowstone, Glacier, Denali and Canyonlands National Parks the inlet height was changed from approximately 3.5 to 10 meters in the mid-1990s. The site at Yellowstone National Park also was moved approximately 1 km. While for many pollutants these changes would be relatively minor, for O_3 this may not be the case. This is because O_3 has a relatively large deposition to the surface, so that during nighttime inversions a significant vertical gradient can result. Thus it is possible that the inlet height change may have an influence on O_3 mixing ratios, especially at night. Given the much stronger vertical mixing, we expect the influence of inlet height on the O_3 mixing ratios will be small during the daytime.

To evaluate the influence from inlet height, we examined the monthly means for daytime (10am-6pm, local time) and nighttime (10pm-6am, local time) O_3 data. We compared data from the same month in the 2 years before and after the inlet change took place. At most parks where this inlet change occurred, the nighttime data showed a jump of several ppbv following the inlet height change. The daytime data did not show any systematic change. This is what would be expected since a strong vertical gradient in O_3 often develops at night. So to ensure that this inlet height change does not influence our analysis, we will focus our trend analysis on only the daytime data. Tables 2.1 and 2.2 show our evaluation of the O_3 data from Yellowstone National Park with respect to inlet height change.

Table 2.1a and b. Monthly mean O_3 mixing ratios for day and night data from Yellowstone N.P. The inlet height was changed from 3.5 to 10 meters in June 1996 (shown in bold font). For each month, we compared the 2 monthly averages for the same month in the two years before and after the inlet change.

2.1a: Daytime O_3 data (10am-6pm), ppbv

Month	1994	1995	1996	1997	1998	Average Change
1		37.0	34.3	36.0	40.9	2.8
2		39.1	37.4	41.4	42.8	3.8
3		52.1	42.3	46.9	47.0	-0.3
4		49.0	44.2	48.1	54.2	4.6
5		50.1	45.6	47.0	51.9	1.6
6	46.9	44.8	**53.3**	47.1	43.5	-0.5
7	45.5	46.6	50.6	44.3		1.4
8	50.6	47.9	50.9	43.1		-2.2
9	45.1	43.9	43.7	38.6		-3.4
10	39.8	40.4	38.3	38.3		-1.8
11	38.2	36.8	33.5	38.8		-1.4
12	38.6	35.5	33.0	37.7		-1.7

2.1b: Nighttime O_3 data (10pm-6am), ppbv

Month	1994	1995	1996	1997	1998	Average Change
1		33.8	31.1	34.7	38.7	4.2
2		33.8	35.3	38.8	40.9	5.3
3		47.2	37.4	43.7	44.5	1.8
4		42.7	38.5	42.9	48.9	5.3
5		36.5	34.1	39.2	44.0	6.3
6	29.3	27.6	**31.1**	35.7	35.3	7.0
7	28.4	23.7	42.5	35.8		13.1
8	32.8	30.4	43.7	34.7		7.6
9	30.3	27.9	36.6	32.8		5.6
10	29.4	32.9	34.3	33.3		2.7
11	32.3	32.0	31.2	34.8		0.8
12	36.6	33.8	32.3	36.3		-0.9

Tables 2.2a and b. Mean difference between O_3 mixing ratios measured before and after inlet height change at Yellowstone N.P. Also shown is the standard deviation of the difference and P-value to evaluate statistical significance.

2.2a: Daytime

Average difference	0.24
SD	2.56
P-value	0.37

2.2b: Nighttime

Average difference	4.91
SD	3.65
P-value	0.00035

The difference was examined between monthly means in the same months for the 2 years before and after the inlet height was changed. June 1996, when the inlet was changed, was excluded from this analysis. This resulted in 12 differences, each of which is calculated from the average 2 months before and after the inlet change took place. A t-test was used to decide if this difference is significant. The analysis shows that the nighttime data were significantly influenced by an average of ~5 ppbv, whereas a difference in the daytime data could not be identified.

John Ray of the National Park Service has also evaluated the influence of inlet height on O_3 at these parks and reached similar conclusions. Dr. Ray's method evaluated the distribution of hourly averages before and after the inlet change and found that this distribution showed a shift away from very low values at night. But he did not see a change in the daytime data (John Ray, NPS, personal communications, 2005).

These data indicate that the nighttime data were influenced by the inlet height change. On the other hand, daytime data either exhibited no influence or the influenced was an inconsequential amount. Other parks, including Rocky Mountain and Lassen showed a similar daytime/nighttime result. We have concluded that the nighttime data are too compromised to reliably use for trend analysis. It should be noted that long-term trends and inter-annual variability complicate this analysis. Nonetheless, these results indicate that the daytime data are most likely not impacted by the inlet change and therefore our trend analysis should focus on the daytime data only.

Detection of trends in geophysical data is complicated by a number of factors, including natural variability and changes in site or operator characteristics. Generally, the greater the natural

variability, the longer it takes to detect a trend (Weatherhead et al., 1998). There are a variety of methods that have been employed to detect trends, some of which are better then others (Hess et al., 2001). In our analysis, we will use least squares analysis on the deseasonalized monthly means, which performs well compared to other methods (Hess et al., 2001). We will also examine results using a multiple regression model which incorporates temperature and biomass burning. Statistical analyses were conducted using SPSS software (Chicago IL) versions 12 and 13.

In this part, we examine the trends using least squares analysis on the deseasonalized monthly means. The results of this analysis are shown in Table 2.3. All trends have been calculated using only daytime data, except for Barrow. For the Rocky Mtn. , Yellowstone and Lassen sites, we also calculated trends using only the data since the inlet height changes were made.

Table 2.3: Trend analysis on deseasonalized monthly mean O_3 mixing ratios. For this analysis only daytime data is used (1000-1800 LST), except for Barrow, where the full dataset was used. For the Rocky Mtn, Yellowstone and Lassen sites, the trends are also calculated using only the data since the inlet height was changed.

Site	Slope (ppbv/year)	R^2	P value	Mean
Rocky Mtn.	0.51	0.22	<0.01	47.2
Rocky Mtn (since 8/1995)	0.55	0.14	<0.01	49.2
Yellowstone	0.50	0.32	<0.01	43.6
Yellowstone (since 7/1996)	0.43	0.13	<0.01	46.1
Lassen	0.33	0.17	<0.01	43.3
(since 8/1995)	0.15	0.01	0.22	44.7
Centennial	0.25	0.13	<0.01	51.1
Canyonlands	0.28	0.11	<0.01	48.0
Craters of the Moon	0.22	0.05	0.01	44.0
Gothic	0.19	0.10	<0.01	51.0
Denali	0.08	0.02	0.06	32.4
Pinedale	0.06	0.01	0.17	49.4
Barrow	0.00	0.00	0.19	26.0
Glacier	0.00	0.00	0.45	32.8

For the two sites in Alaska, no significant trend is apparent. Of the 9 sites in the continental U.S., 7 have a statistically significant positive trend, with slopes ranging from 0.51-0.19 ppbv/year. No site has a negative trend. The average slope for the 9 continental U.S. sites, including the two with no significant trend, is 0.3 ppbv/year. For Rocky Mtn., Yellowstone and Lassen, the trends since the mid-1990's are similar to the trends calculated using the entire data record, which indicates that the change in inlet height is not likely the reason for these trends. These results imply that for the 17 year period (1988-2004) rural-remote O_3 in the western U.S. has increased by approximately 5 ppbv. In the next section we will analyze the O_3 trends by season and examine its relationship to temperature.

For the sites with the strongest long-term trend and data records going back into the late 1980s (Rocky Mountain, Yellowstone, Lassen and Centennial), we examined the seasonal pattern for the O_3 trend. Daytime, hourly data were averaged into a seasonal mean value. Winter included the months of December, January and February, and other seasons were defined accordingly. Data from December was included with data from January and February of the next year. The results are shown in Table 2.4 for these four parks.

Table 2.4: Seasonal trends in daytime O_3 mixing ratios.

	Slope (ppbv/year)	**R^2**	**P value**
Rocky Mtn.			
Winter	0.62	0.32	0.01
Spring	0.59	0.32	0.02
Summer	0.50	0.20	0.07
Fall	0.32	0.20	0.06
Yellowstone			
Winter	0.56	0.53	0.01
Spring	0.38	0.19	0.08
Summer	0.49	0.39	<0.01
Fall	0.56	0.63	<0.01
Lassen			
Winter	0.21	0.19	0.08
Spring	0.33	0.41	0.01
Summer	0.43	0.31	0.02
Fall	0.28	0.17	0.12
Centennial			
Winter	0.39	0.56	<0.01
Spring	0.30	0.39	0.04
Summer	0.22	0.07	0.02
Fall	0.15	0.08	<0.01

Since there are now many fewer data points, the P-values tend to be higher. However, there is no clear pattern in either the slopes or R^2 values. The slopes are positive in all seasons and most are significant, with P values <0.05. We conclude from this that the O_3 trends are relatively uniform throughout the year.

3. Influence of temperature on O_3 trends

Because of the importance of temperature on O_3 production, we have evaluated whether temperature changes may be responsible for some of the ozone trends we see. To do this, we used the observed temperatures at each site in a multiple regression model. This is functionally equivalent to applying a meteorological adjustment, but we prefer this direct method as it provides a better accounting of the factors responsible for the observed O_3 concentrations, without changing the actual concentrations. To do this we start with a linear expression which expresses the O_3 concentration as a function of multiple factors:

$$\textbf{Observed } O_3 = \textbf{seasonal factor + temperature factor + trend + residual}$$

To quantify each component in this expression, we first calculate the departure from the monthly mean temperatures. The monthly mean temperature departure is then used in a linear regression model, along with time, as a predictor on the deseasonalized monthly mean O_3 concentrations:

$$\delta O_3 = A_1 * \Delta\text{temp} + A_2 * \text{time} + \text{residual}$$

Where:

δO_3 is the deseasonalized daytime, monthly mean O_3 mixing ratio;

Δtemp is the monthly temperature departure from the mean

A_1 and A_2 are coefficients determined from the regression.

Note that the difference between the monthly mean departure and the deseasonalized monthly mean values is simply the annual average. Either value could be used in the regression model, the final results are identical. We did this separately for the warm season (May-September) and cold season months. Not surprisingly, we found that temperature is not a useful predictor for O_3 concentrations during the colder months. Table 3.1 shows the results for the warm season

months. For comparison, Table 2.4 shows the summer trend analysis without including temperature.

Table 3.1. Results from two variable regression model, which uses temperature and year as predictors for the deseasonalized daytime monthly mean O_3 for the months of May-September. All regressions are statistically significant at P<0.01. Values in parentheses give the P value for that coefficient.

Site	Temperature coefficient-A1 (ppbv/oC)	Trend coefficient-A2 (ppbv/year)	R^2
Rocky Mtn.	1.3 (<0.01)	0.46 (<0.01)	0.26
Yellowstone	0.27 (0.20)	0.45 (<0.01)	0.53
Lassen	0.74 (0.02)	0.36 (<0.01)	0.27

While the overall R^2 for these regressions is improved compared to the model without temperature, the trend coefficients have changed very little. In all cases, the trend coefficient (A_2) remains statistically significant. These results indicate that temperature changes do not explain most of the observed trend in O_3.

4. Use of HYSPLIT backward trajectories to segregate Rocky Mtn N.P. O_3 data

To evaluate the influence of transport on O_3 at Rocky Mountain National Park, we have used back-trajectories to segregate the dataset. For this we calculated daily HYSPLIT back-trajectories for the period 1990-2004 using the NCEP Reanalysis meteorological data. Trajectories were calculated back for 1 and 5 days. The trajectories were clustered using a non-hierarchical k-means algorithm. In other words, each day's transport was classified according to the cluster or transport type. By definition, cluster A is the shortest grouping and represents local/regional transport. Cluster F is the longest cluster group and represents transport from greater distances in the same 24 hour period. It should be noted that the NCEP Reanalysis has a horizontal grid spacing of 2.5^o x 2.5^o. Thus we were not sure how well the trajectory analysis would work in mountainous regions where this grid spacing does a poor job of capturing the true terrain heights. Figure 4.1

shows an example of one trajectory from Cluster A, and Figure 4.2 shows one trajectory from Cluster F.

Figure 4.1: One day back-trajectory for Rocky Mountain National Park on June 9, 2004 with an arrival time of 18 GMT. This trajectory was calculated using the NOAA-HYSPLIT model, with the NCEP Reanalysis meteorological data and model vertical velocities. This trajectory was included in Cluster A, which contains trajectories showing the slowest 24-hour transport. The arrival coordinates are 40.28°N 105.55°W and we used an arrival altitude of 500 meters above model ground level, which corresponds to approximately 2800 meters above sea level. The daily maximum 8-hour O_3 concentration for this day was 61 ppbv.

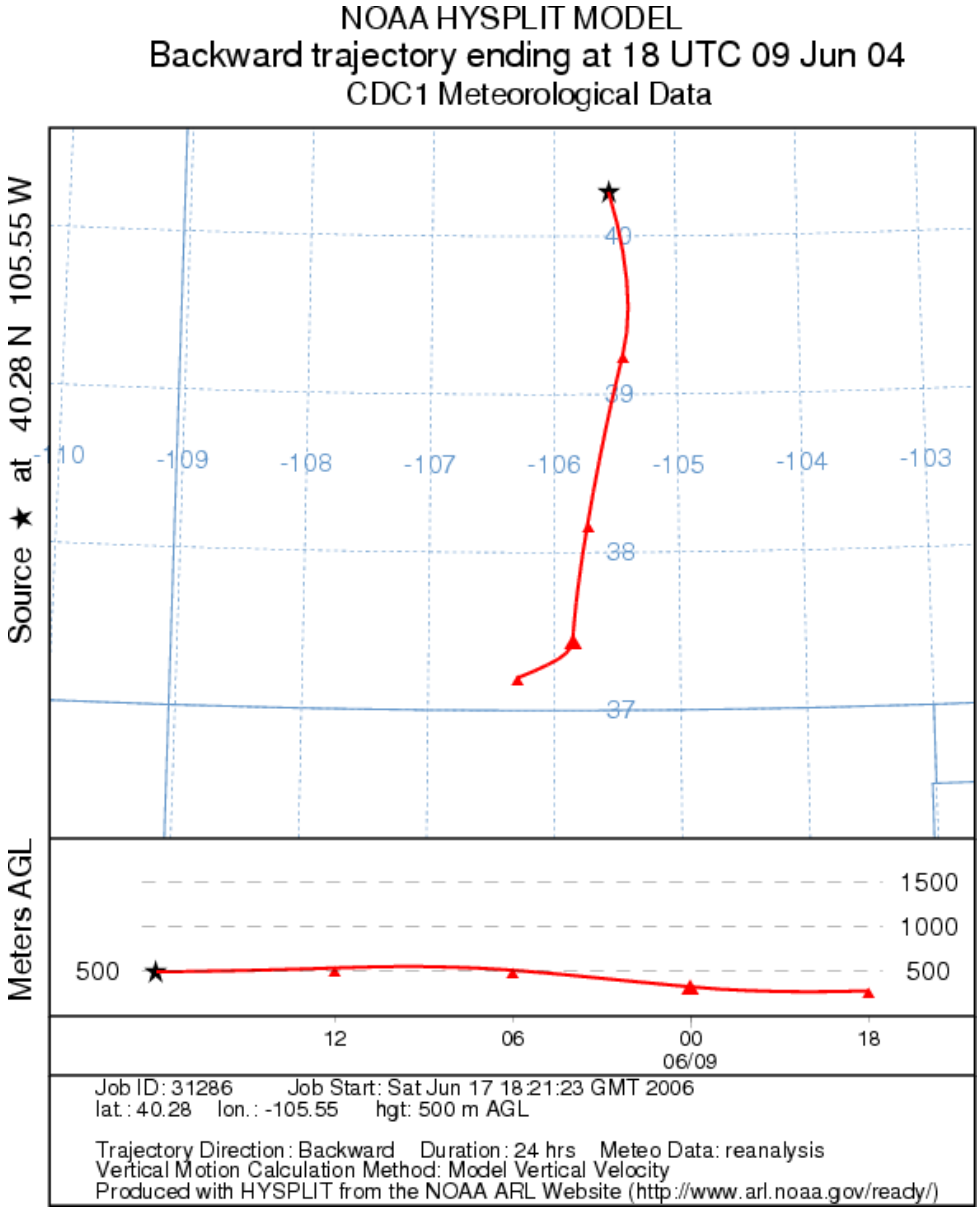

Figure 4.2: One day back-trajectory for Rocky Mountain National Park on May 27, 2004 with an arrival time of 18 GMT. This trajectory was calculated using the NOAA-HYSPLIT model, with the NCEP Reanalysis meteorological data and model vertical velocities. This trajectory was included in Cluster F, which contains trajectories showing faster 24-hour transport. The arrival coordinates are 40.28°N 105.55°W and we used an arrival altitude of 500 meters above model ground level, which corresponds to approximately 2800 meters above sea level. The daily maximum 8-hour O_3 concentration for this day was 53 ppbv.

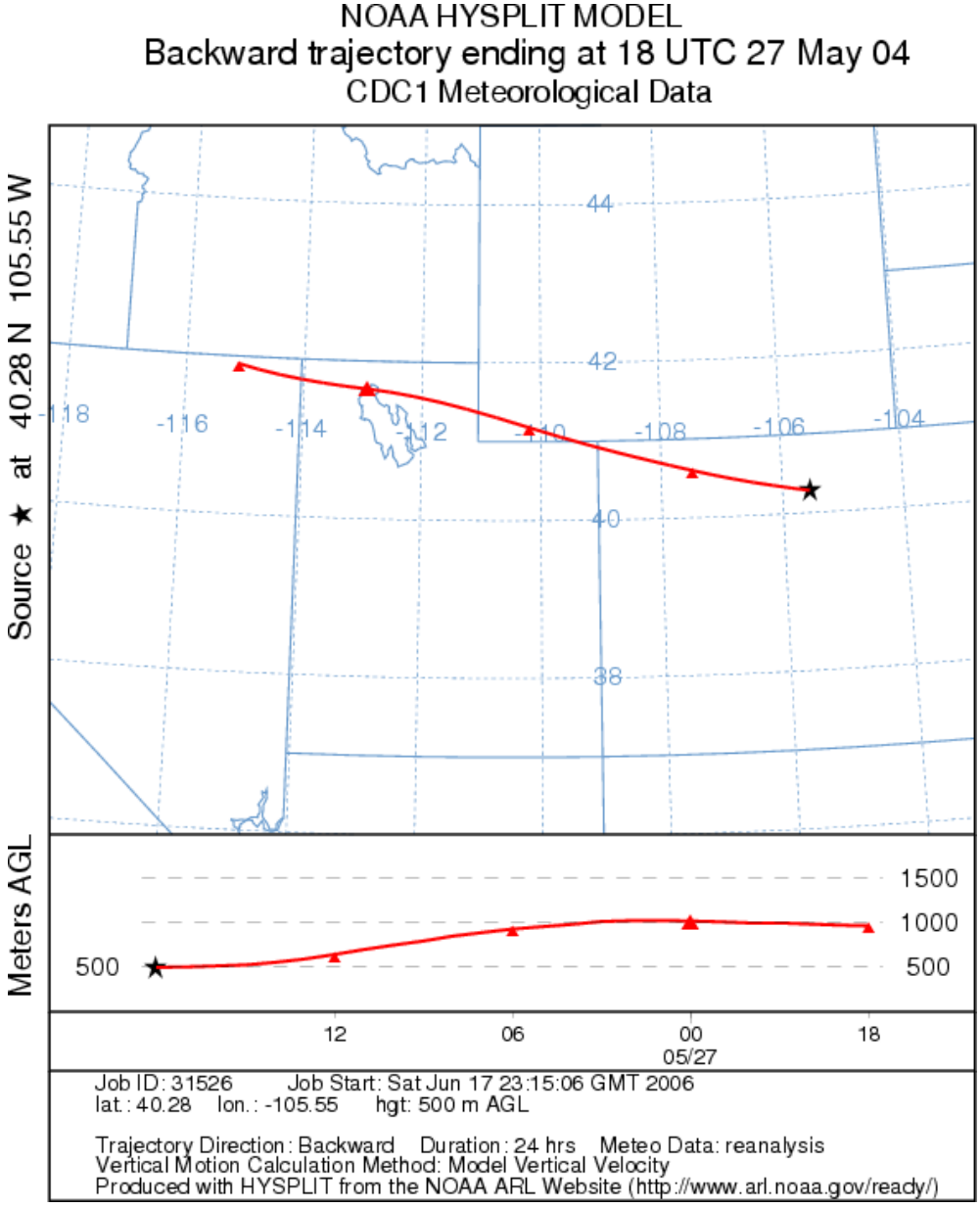

The air mass arriving at Rocky Mtn. N.P. on May 27, 2004 had traveled approximately twice as far in the previous 24-hours, compared to the air mass that arrived on June 9, 2004. Also, for this example, the daily maximum 8-hour O_3 concentration for May 27, 2004 was significantly lower than for June 9, 2004. Note that while the trajectory in Figure 4.1 shows transport from the more populated regions of Colorado, not all Cluster A trajectories show this same characteristic. But they do all exhibit weaker flow and slower transport, which is characteristic of stagnant conditions. Cluster A trajectories also generally show greater influence from near surface air (compare the elevation history of the air mass in Figures 4.1 with the air mass in Figure 4.2). The clustering algorithm we use largely separates the trajectories based on distance traveled and the transport direction. Clusters B, C, D and E represent intermediate cases between the extremes of clusters A and F.

Table 4.1 below shows the average 8-hour daily maximum O_3 mixing ratio, sorted by cluster type (based on 1-day back trajectories) for the 15-years of data in this analysis.

Table 4.1: Mean 8-hour daily maximum O_3 concentration vs cluster type, number of days in each cluster (N) and standard deviation for each cluster using 1-day back trajectories (1990-2004 data). Cluster A shows the shortest transport and Cluster F the longest.

Mean 8 hr daily max (ppbv)	Winter	Spring	Summer	Fall
Cluster A	42.88	53.01	57.87	47.05
Cluster B	45.00	53.07	56.57	43.94
Cluster C	45.44	55.75	57.53	47.41
Cluster D	44.73	57.70	56.88	45.51
Cluster E	45.43	52.67	55.89	45.36
Cluster F	45.44	54.61	52.86	44.67
N	**Winter**	**Spring**	**Summer**	**Fall**
Cluster A	76.00	187.00	473.00	227.00
Cluster B	145.00	235.00	223.00	163.00
Cluster C	266.00	342.00	401.00	390.00
Cluster D	193.00	218.00	137.00	204.00
Cluster E	285.00	190.00	33.00	230.00
Cluster F	248.00	98.00	16.00	127.00
S.D. (ppbv)	**Winter**	**Spring**	**Summer**	**Fall**
Cluster A	5.77	9.44	11.92	10.98
Cluster B	5.70	7.82	10.80	9.75
Cluster C	4.52	7.33	10.08	7.80
Cluster D	5.59	7.51	10.63	8.70
Cluster E	4.14	7.18	10.13	5.06
Cluster F	3.93	6.50	7.96	5.80

Using the 1-day trajectories, we find that for summer there is a tendency for higher ozone concentrations on days with shorter back-trajectories (e.g., Cluster A or B). Figure 4.3, below, shows the mean daily maximum O_3 concentration for summer months averaged by cluster type.

Figure 4.3: Daily 8-hour maximum O_3 concentration for summer, averaged by cluster type (1990-2004 data). Cluster A is the shortest grouping and Cluster F the longest.

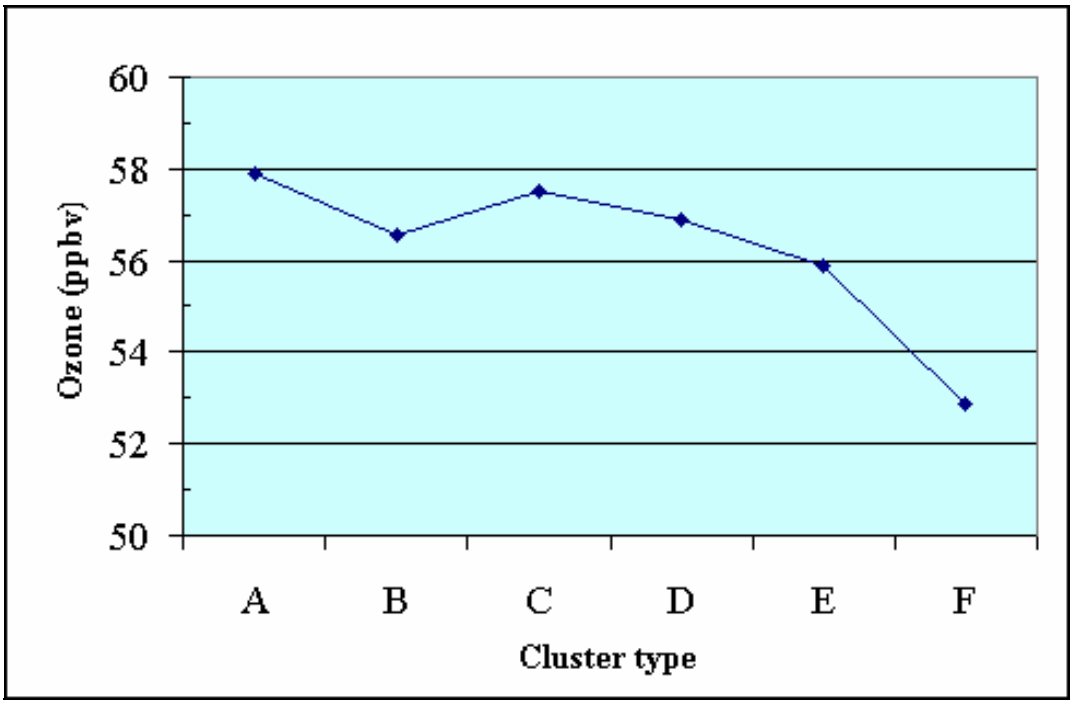

However, it should be noted that not all of these differences are statistically significant. For example, the difference between the summer means for Clusters A and C is only 0.34 ppbv and this difference is not statistically different. However, the difference between Clusters A and F is 5.01 ppbv, which is statistically significant. In general these results are not surprising: days with greater stagnation leads to higher O_3 concentrations.

We also examined the same relationship as those above, but using 5-day back trajectories. The results are shown in Table 4.2 below.

Table 4.2: Mean 8-hour daily maximum O_3 concentration vs cluster type, number of days in each cluster (N) and standard deviation for each cluster using 5-day back trajectories (1990-2004 data). Cluster A shows the shortest transport and Cluster F the longest.

Mean 8 hr daily max (ppbv)	Winter	Spring	Summer	Fall
Cluster A	44.32	54.27	57.18	46.62
Cluster B	46.62	52.36	56.71	42.29
Cluster C	45.02	56.67	57.75	47.23
Cluster D	45.14	54.26	57.36	46.24
Cluster E	45.05	54.04	56.81	44.37
Cluster F	46.38	54.75	ND	45.61
N	**Winter**	**Spring**	**Summer**	**Fall**
Cluster A	216.00	266.00	590.00	410.00
Cluster B	40.00	140.00	111.00	78.00
Cluster C	238.00	312.00	353.00	243.00
Cluster D	289.00	334.00	207.00	351.00
Cluster E	316.00	166.00	22.00	171.00
Cluster F	114.00	52.00	0.00	88.00
S.D. (ppbv)	**Winter**	**Spring**	**Summer**	**Fall**
Cluster A	5.70	8.64	11.00	9.61
Cluster B	5.41	7.43	12.40	9.90
Cluster C	5.01	8.09	10.87	8.41
Cluster D	4.80	7.14	10.31	7.52
Cluster E	3.96	7.66	9.73	6.03
Cluster F	3.85	7.52	ND	6.22

Using the 5-day back trajectories to segregate the data, we find that the mean of the daily maximum O_3 values does not show the same pattern as using the 1-day back trajectory clusters. This reflects much poorer air mass segregation using the 5-day back trajectories. For this reason, we will only consider further the clusters generated from the 1-day back trajectories.

Knowing that the 1-day back-trajectories can reasonably segregate the air mass transport history, we can evaluate the trends by transport regime or cluster type. Using the 1-day clusters, we

can then examine the O_3 trends that we have reported previously. Table 4.3 shows the 15-year O_3 trends separated by season and 1-day trajectory clusters.

Table 4.3: Trend in mean daily 8-hour maximum O_3 concentrations segregated by season and cluster type (1990-2004 data) using 1-day back trajectories.

Season	Cluster	Slope	R^2	P value
Winter	A	0.406	0.26	0.05
Winter	B	0.577	0.57	<0.01
Winter	C	0.525	0.69	<0.01
Winter	D	0.679	0.65	<0.01
Winter	E	0.530	0.66	<0.01
Winter	F	0.397	0.61	<0.01
Spring	A	0.432	0.18	0.13
Spring	B	0.323	0.12	0.22
Spring	C	0.510	0.34	0.03
Spring	D	0.420	0.42	0.01
Spring	E	0.369	0.19	0.12
Spring	F	0.505	0.31	0.05
Summer	A	0.688	0.235	0.08
Summer	B	0.770	0.21	0.10
Summer	C	0.622	0.20	0.11
Summer	D	0.514	0.12	0.23
Summer	E	Insufficient data		
Summer	F	Insufficient data		
Fall	A	0.785	0.38	0.02
Fall	B	0.579	0.22	0.08
Fall	C	0.667	0.55	<0.01
Fall	D	0.475	0.25	0.06
Fall	E	0.442	0.29	0.04
Fall	F	0.577	0.50	<0.01

From this analysis no clear pattern emerges. As reported previously (Jaffe, CRC 2005), the trends are present in all seasons, somewhat less so in summer according to this analysis. There does not appear to be any relationship between the transport cluster and the observed trends. In other words, the O_3 increases appear to be broadly present and not confined to local air masses.

Probably the most important factor in this analysis is the resolution of the meteorological data. The relatively poor resolution (2.5^o x 2.5^o) in regions of mountainous terrain result in large uncertainties associated with trajectory calculations. Unfortunately, we are not aware of any finer resolution meteorological data that extends over a sufficiently long time period.

5. Use of Boulder ozonesonde data to evaluate free tropospheric trends

The broad pattern of increasing O_3 in the western U.S. suggest a large scale phenomena. For this reason we also sought to examine whether an O_3 increase could be identified from any free tropospheric datasets in the region. The National Oceanic and Administration (NOAA) has made ozonesonde measurements at two sites in the western U.S.: Boulder, Colorado (since 1979) and Trinidad Head, California (since 1997). However, the shortness of the Trinidad Head record prohibits a trend analysis. Therefore, we have examined only the Boulder data for trends. Between 1979-2003, there have been 909 ozonesonde launches, but these have not been evenly spaced. In some years, there were only 9 ozonesonde launches while in other years there were as many as 56. Generally, there were fewer launches in the early part of the data record, with a significant increase in the number of launches starting in 1985. It should also be noted that ozonesondes are subject to interferences (especially SO_2) and launch procedures have been changed (e.g., ECC cathode solution). Both of these issues make trend determination from ozonesondes more problematic than from surface UV measurements.

Boulder (population ~100,000) is located is in the foothills of the Rocky Mountains of Colorado at an elevation of 1.7 km. It is adjacent to the Denver metropolitan area and so frequently experiences episodes of elevated O_3. While the local influence will dominate the boundary layer in this region, it may also be important at higher elevations due to convection. For our analysis of the ozonesonde data, we segregated the data into 3 bins: boundary layer (below 4.0 km asl), lower free troposphere (4.0-8.0 km asl) and upper free troposphere (8.0 -12.0 km asl). Layers with O_3 mixing ratios greater then 100 ppbv are likely due to stratospheric air or a substantial pollution influence and were excluded from the analysis. Because of the small number of sondes in earlier years, we

only evaluated the trends from 1985-2003. This includes 837 ozonesondes, for an average of 44 sondes/year (none launched between December 1989 and June 1991). Trends for each season were examined separately. We analyzed the ozonesonde data by calculating Deseasonalized Monthly Means (DSMM) for the 3-8 km ozone mixing ratios. Figure 5.1, below, shows the DSMM for the 3-8 km mean O_3 mixing ratio from 1985-present. The R^2 for the linear fit is 0.02, so clearly no significant trend is present in these data. A similar result was found (no trend) if the data was examined in separate layers, e.g. 3-5 km, and 5-8 km.

Figure 5.1: Deseasonalized monthly means for 3-8 km from the Boulder ozonesonde data.

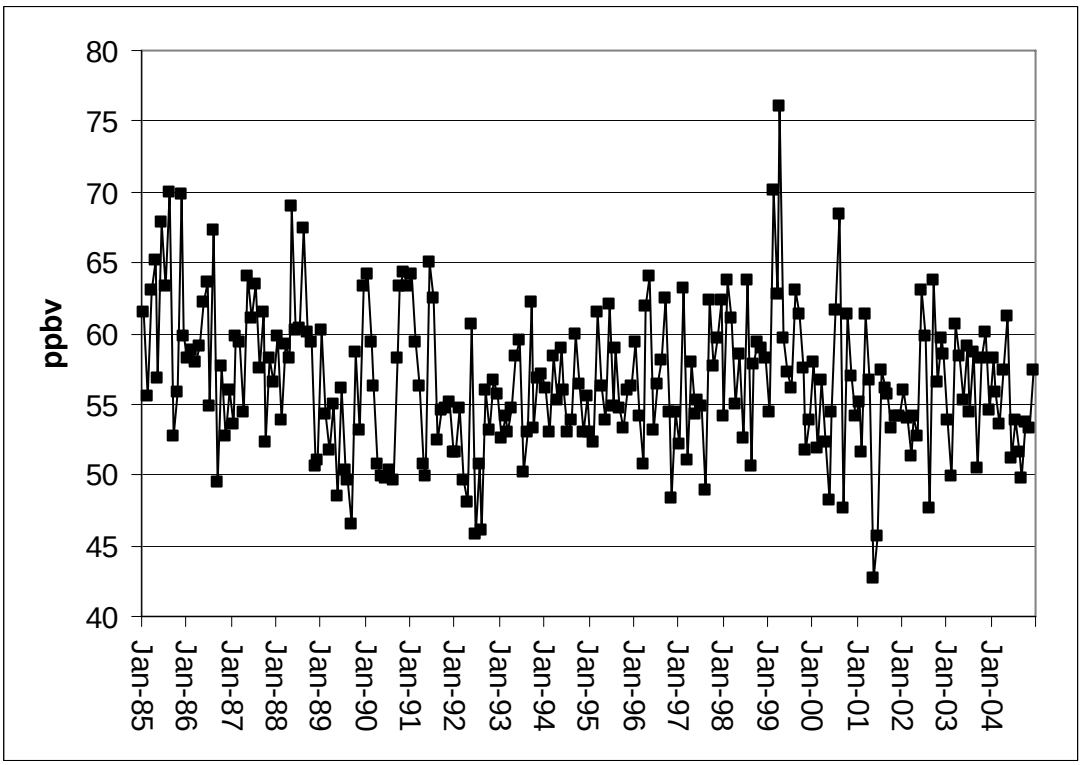

For the boundary layer, we found a statistically significant decrease in O_3 for winter, spring and summer, with slopes ranging from 0.2-0.4 ppbv/year. This is in contrast to results from the continuous surface monitoring in Boulder, Colorado, which shows a noisy, but positive trend in the annual 4th highest 8-hour O_3 concentration (CDPHE 2004). While these measures are different, summer mean vs 4th highest 8-hour concentration, we would expect a similar pattern in the trends. This suggests that the small number of ozonesonde launches per month, averaging less then 4, does not give a good representation of the monthly mean O_3 concentrations.

Overall, the Boulder ozonesonde data do not indicate a trend in free tropospheric O_3. However, the relatively small number of ozonesondes and the uneven temporal distribution of these data make trend analysis somewhat ambiguous. This is especially so given the disagreement between the trends found from the Boulder surface monitoring site and the boundary layer ozonesonde data. Thus our conclusion regarding the lack of a free tropospheric trend should be considered preliminary.

Many researchers have used ozonesonde data to evaluate possible long-term trends. However, the results are highly variable, with large apparent shifts in the trends from one region to another and over relatively short time spans. So, we sought to examine the ozonesonde data in more depth by comparing against continuous surface O_3 monitoring data. This will allow us to examine the following questions:

1) Is there any evidence for bias between the surface UV and ozonesonde data?
2) How does the precision of the two methods compare?

The Boulder data appear to be nearly ideal for this comparison. This is because we have a long term ozonesonde record, along with nearby surface O_3 measurements by UV.

Datasets used:

1) NOAA-CMDL ozonesonde for Boulder, CO
2) South Boulder monitoring station (1405½ South Foothills Highway, approximately 1 km NW of Marshall)
3) Rocky Flats surface monitoring station (16600 W. Colorado Hwy 128, near Boulder County-Jefferson County border)

These sites are all within about 10 km of each other, with the ozonesonde launch site located between the two surface monitoring locations.

The hourly surface UV O3 data are from the regional/state air quality network. Time in these datafiles is local standard time. The data were obtained from the EPA AIRS database and the state of Colorado. For both the sondes and surface data, we used all data between June 1994-December 2004. The Rocky Flats dataset has very little missing data, whereas the S.Boulder monitoring site has about 14 months of missing data over this time period.

Data selection:

For the ozonesonde data, we used data from the "250 meter" datafiles obtained from the NOAA-CMDL monitoring lab's website (www.cmdl.noaa.gov):

bld_1979-2003_normalized-SBUV.lvl

bld_2004_normalized-SBUV.lvl

To compare with the nearby surface observations, we used data from the first level in the file (Level =1) and also the mean of the first 2 levels (Level=1,2). This should represent the air sampled by the sonde during the last few minutes before launch (Level=1) or the lowest 250 meters (Level=1,2), respectively. For the surface data, we used the hourly value which included the sonde launch time. The sonde and UV data were formatted to UTC for comparison.

Point by point comparison

Figure 5.2 shows a point by point comparison of sonde and UV data for times when there was simultaneous UV and ozonesonde data. During this 11 year period, there were approximately 520 ozonesonde flights. However, due to missing UV data, there are only 437 points with simultaneous UV and sonde data. Because of the small number of datapoints at low concentrations, the regression fit is quite uncertain at the low end. We found that it made almost no difference whether the sonde data from only the lowest layer (Level =1) or the lowest 250 meters (average of Levels =1,2) was used.

Figure 5.2: Scatterplot of sonde data (Level 1) vs UV O_3 data from South Boulder monitoring station for the same hour as the sonde launch time. No difference was found if we used an average of sonde Levels 1 and 2.

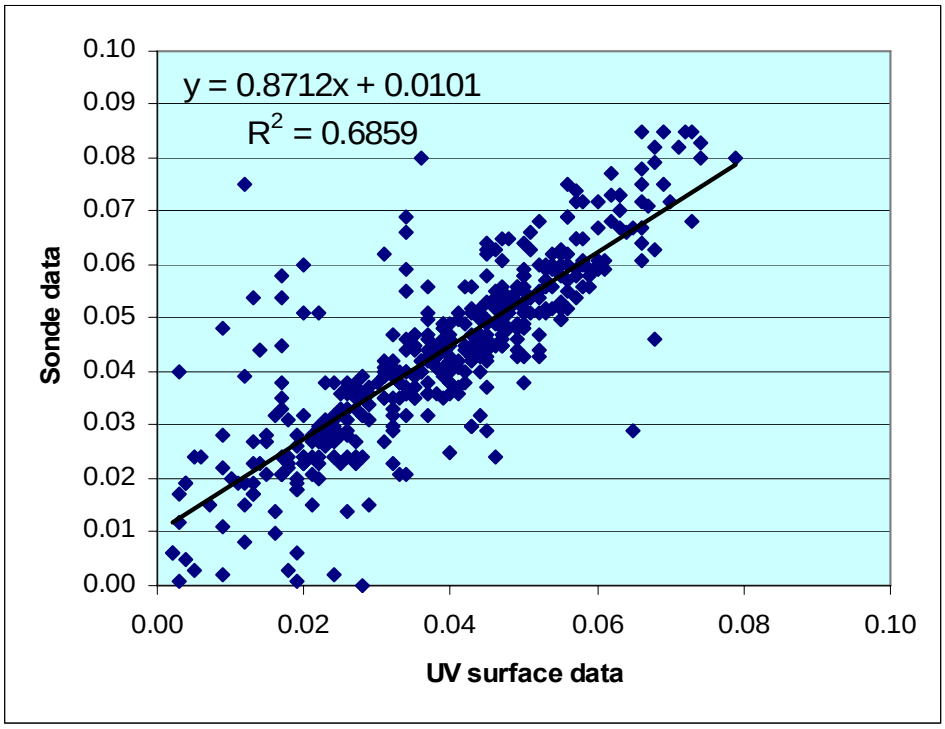

If we force the regression fit through zero, we get a slope of 1.11, with a R^2 of 0.631. For the dataset as a whole, the RMS difference is 0.011 ppmv. Looking at just the low points (<0.02 ppmv) there is no evidence for bias between the measurements, although there is more scatter (RMS difference = 0.018 ppmv). The greater scatter at low concentrations is probably due to greater uncertainties in the measurements as well as larger spatial and temporal variations at low concentrations.

Comparison of monthly means

To evaluate long-term trends, we often use monthly or annual means to reduce daily variability. To compare the ozonesonde and UV O_3 measurements, we will examine monthly means using several approaches. Figure 5.3 below shows a comparison of the monthly means calculated for each dataset using only times with simultaneous data.

Figure 5.3: Scatter plot of monthly means from sonde data (Level 1) and UV O_3 measurements. For this plot, we computed monthly means using only the simultaneous points. Each monthly mean is an average of between 1-8 sonde datapoints and 1-8 hours of surface data per month. Clearly the sonde data give a very good representation of the monthly mean concentration during these time periods with three exceptions (February, March, April 1999). If the Februray-April 1999 points are excluded, the regression equation becomes y = 0.9988x + 0.0046, with an R^2 of 0.843.

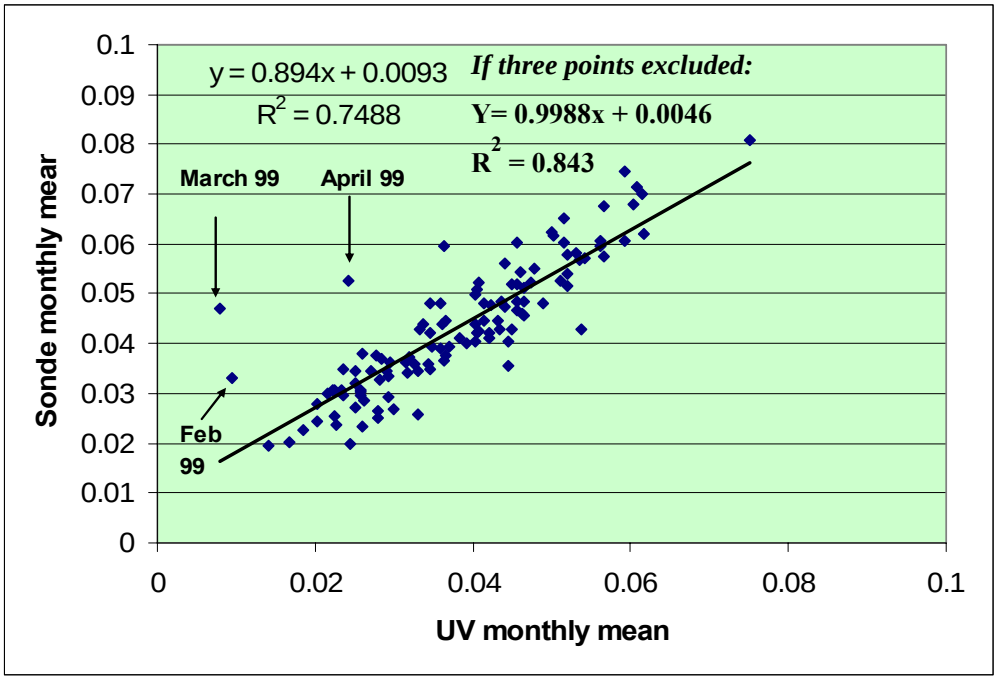

With the exception of three months, the comparison is excellent. For these three months, February, March and April 1999, the surface UV O_3 mixing ratios are exceptionally low. This is true both for the UV data associated with the sonde launch times, as well as the overall monthly means. Because this suggests some problem with the UV data during those months, we will exclude these months from all further analysis. We went back and re-examined the point-by-point comparisons above, but because of the much larger number of individual datapoints, excluding the Feb-April 1999 datapoints has little influence on the analysis. If we exclude the monthly means from Feb-April 1999, the regression equation becomes: y = 0.9988x + 0.0046, with an R^2 of 0.843. The RMS difference for these monthly means is 0.007 ppmv.

However, a typical month includes only 1-8 sonde launches. Now we want to see whether the monthly mean for these data points is a good reflection of the true monthly mean. Figure 5.4 below shows this comparison.

Figure 5.4: Comparison of monthly means from sonde data (1-8 launches per month) with all monthly data from UV measurements.

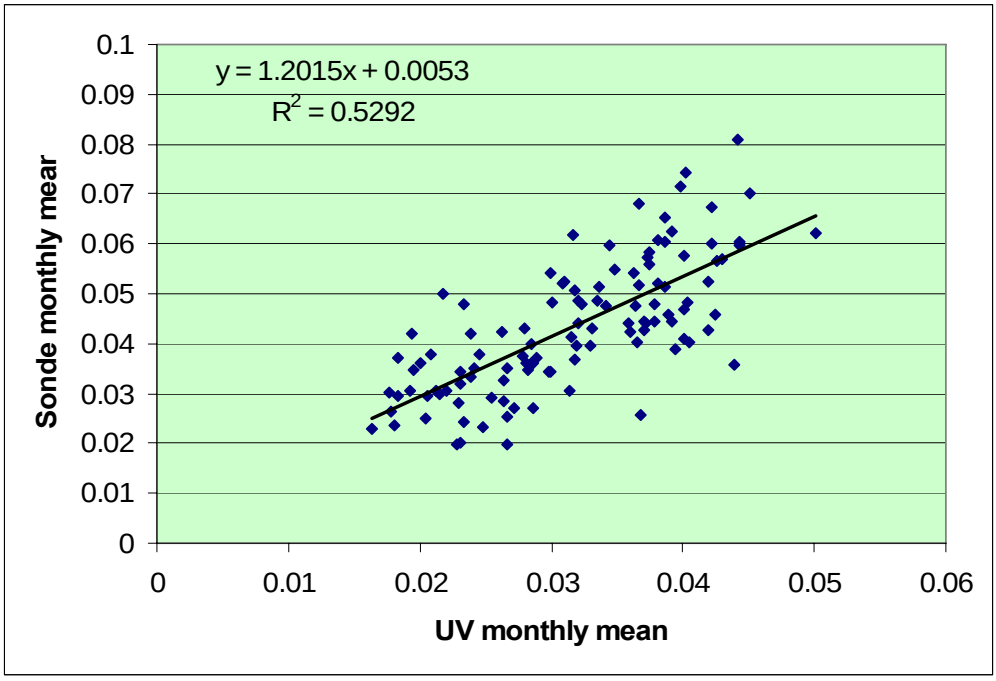

From the figure we see that the comparison is significantly worse. The R^2 has dropped substantially and the RMS difference is now 0.015 ppmv. Also, the regression line suggests a significant bias between the sonde data and the UV data. One possible explanation for this is the diurnal cycle of O_3, since the sondes are always launched during daytime, when O_3 is usually higher. This is examined in the Figure 5.5 below.

Figure 5.5: Comparison of monthly means (mm) from sonde data (1-8 launches per month) with monthly means calculated using only daytime (1000-1800 LST) UV measurements from S. Boulder surface monitoring site. The linear regression and 1:1 lines are shown as solid and dashed lines, respectively.

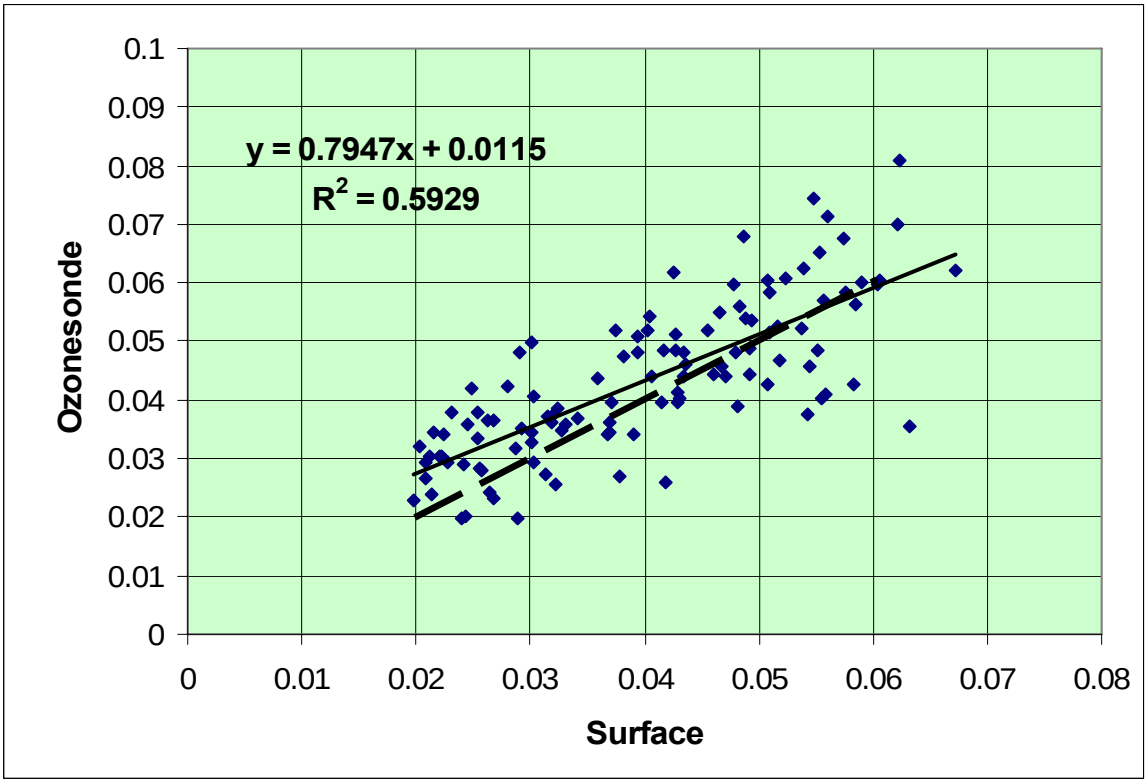

This figure shows that the agreement between sonde monthly means and UV monthly means improves if we only use the daytime UV data, although there is some evidence for an offset at low monthly means. The RMS difference for this comparison is 0.009 ppmv. We also did the same comparison with the Rocky Flats surface, daytime O_3 data and found a similar result (y = 0.7736x + 0.0089, R2 = 0.6306, RMS difference = 0.008 ppmv).

Finally, shown below in Figure 5.6 is a time series of the daytime monthly mean O_3 concentrations, as measured by the sonde and the UV instrument, for the South Boulder site for the 1994-2004 timeframe using all data for each dataset, respectively.

Figure 5.6: Daytime monthly mean O_3 concentration (ppmv) from Boulder sondes and surface UV data. For both datasets, all valid daytime data is used to compute the monthly mean.

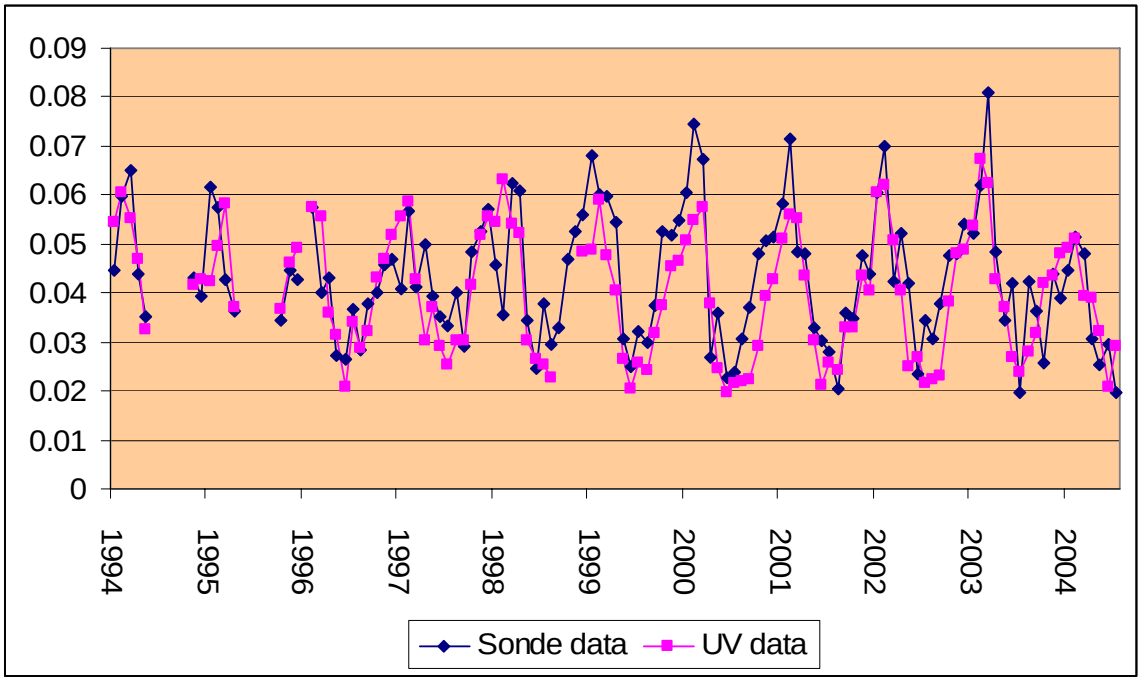

In summary, it seems that the individual points and monthly means show no evidence for bias. However, because O_3 is highly variable in time, the number of datapoints per month will significantly influence our ability to detect trends. So next we address whether or not the 4 ozonesonde launches per month is adequate to evaluate long-term trends.

Data from Rocky Flats UV O_3 monitoring site

Using data from the Rocky Flats UV O_3 monitoring site will allow us to examine whether some of these differences are due to spatial variability. By comparing the monthly means from S.Boulder, with Rocky Flats data and the ozonesonde data, we can examine this variability. This is shown in Figure 5.7 below.

Figure 5.7: Comparison of monthly mean O_3 concentration from the two UV O_3 monitoring sites, South Boulder and Rocky Flats.

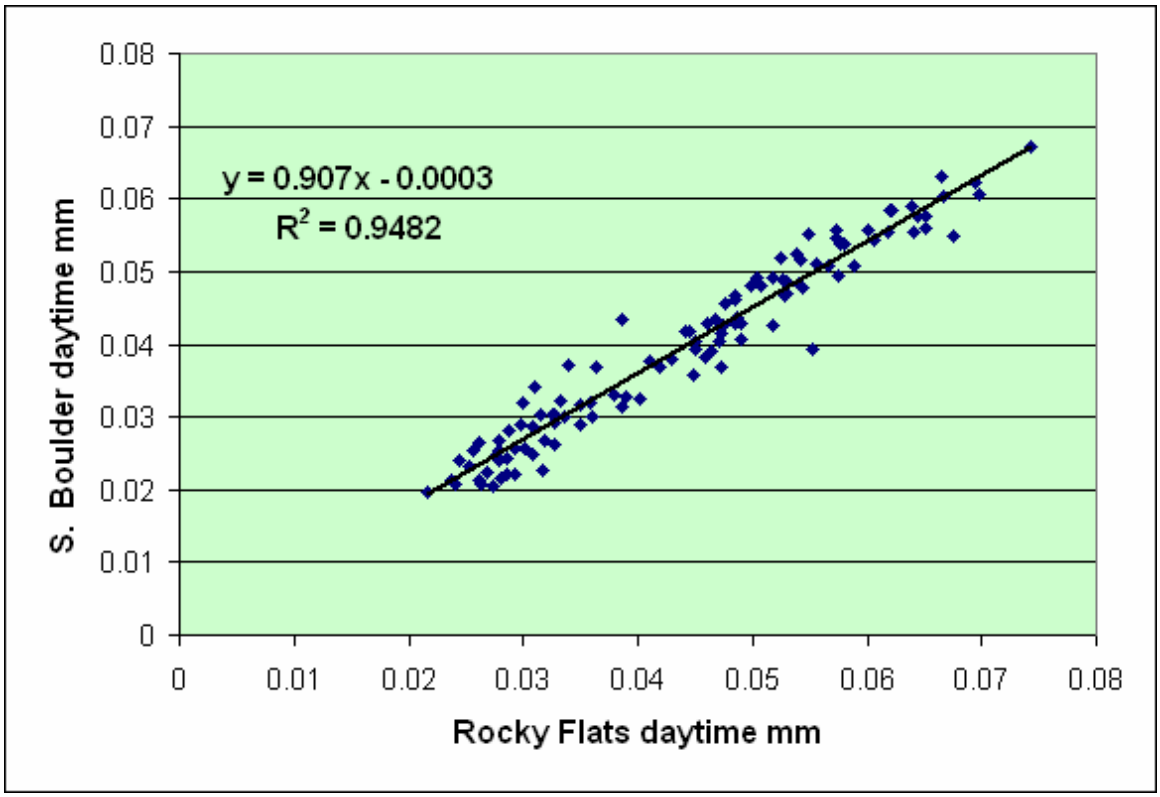

The comparison between the two nearby surface sites is excellent. Although there appears to be some real difference in O_3 mixing ratios at the two sites, the month to month variations are correlated very well at the two sites.

Figure 5.8, below, shows the comparison of ozonesonde monthly means with the Rocky Flats daytime monthly means. The comparison shows significantly more variability then the two surface monitoring sites.

Figure 5.8: Comparison of monthly means from sonde data (1-8 launches per month) with monthly means calculated using only daytime (1000-1800 LST) UV measurements from Rocky Flats surface monitoring site.

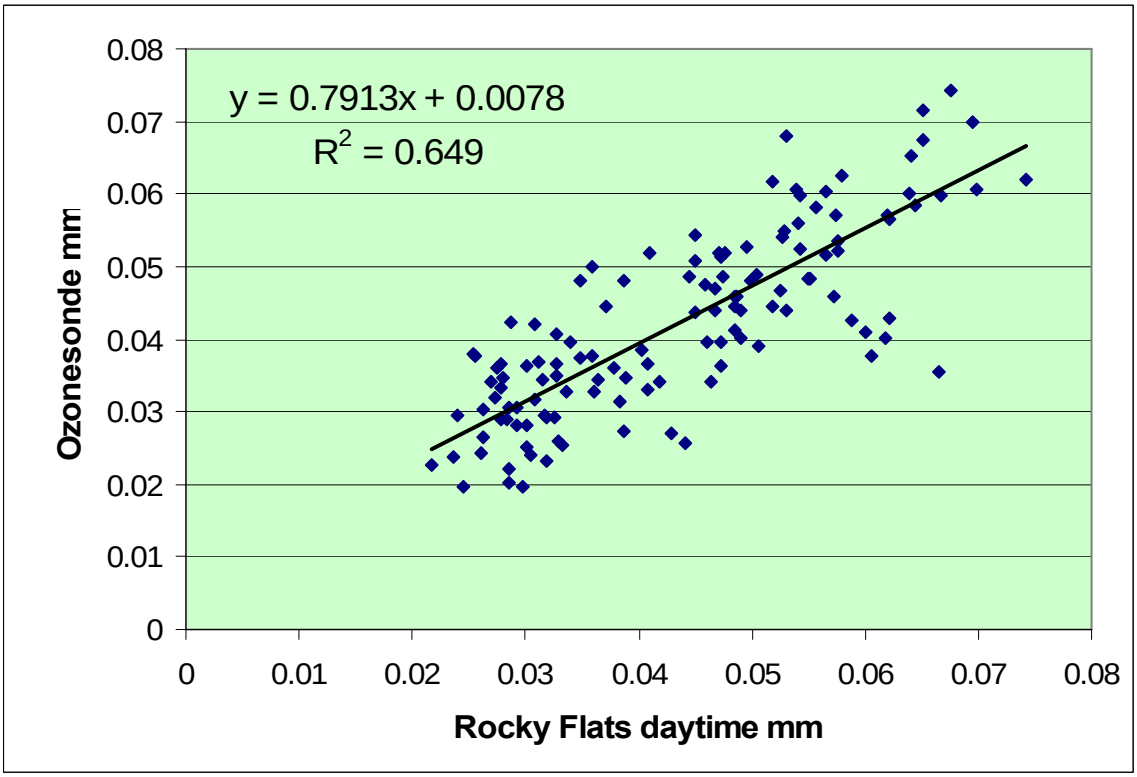

Trend Detection

We now turn our attention to how well the sonde data can detect trends, as compared to the continuous monitoring data. This analysis is based on work by Tiao et al. (1990) and Weatherhead et al. (1998, 2000). The essential model is as follows:

Y(t) = Mean + Seasonal component + Trend component + Noise

Where Y(t) represents the monthly mean values and where the noise component may include an auto-regressive term.

As shown by Tiao et al. (1990) and Weatherhead et al. (1998, 2000), the ability to detect trends depends on two factors, the variance and autocorrelation in the noise component. To evaluate the trend detection capabilities, we evaluated these two factors for the sonde and surface UV ozone observations.

For each dataset, we computed daytime monthly means, this includes all sonde data, but only daytime surface UV observations. Each dataset was deaseasonalized using the SPSS

"Seasonal Decomposition" procedure, which adds or subtracts a Seasonal Adjustment Factor (SAF). The SAF is calculated from the difference between the monthly mean for each month for all years and the mean for the entire dataset. The resulting datasets were then investigated for variance and autocorrelation.

Table 5.1: Mean (ppmv), standard deviation, relative standard deviation, auto-correlation and trend detection time are given in the table below basd on the deseasonalized monthly means (DSMM). The number of years to detect a trend is based on Equation 3 of Weatherhead et al (1998).

	$\overline{X}$ (ppmv)	σ_{dsmm} (ppmv)	RSD	Auto-correlation	Years to detect trend of 0.5%/year	Years to detect trend of 1%year
Boulder-ozonesdones Layer 1	0.0424	0.0077	18.2 %	0.143*	26.8-34.0	16.9-21.4
Rocky Flats surface UV O_3 data (daytime only)	0.0437	0.0041	9.4 %	0.356	20.1	12.7
S.Boulder surface UV O_3 data (daytime only)	0.0400	0.0056	14.0	0.464	28.6	18.0

* We have assumed that the true auto correlation is given by the surface UV data. The larger noise level inherent in the ozonesonde data appears to obscure the autocorrelation. For this reason, we have used the ACF value of 0.464 for the ozonesonde calculations. If instead we use the ozonesonde ACF value (0.143) then the years to detect the trends are 26.8 and 16.9 years for 0.5%/year and 1%/year trends, respectively, for the ozonesonde dataset.

Conclusions concerning ozonesondes

We compared the balloon borne ozonesonde observations with continuous surface O_3 measurements taken nearby during the period when the balloon was in the surface layer. The three datasets have been compared in multiple ways. When we select only those time periods with simultaneous ozonesonde and surface observations and do a point by point comparison, we find a reasonable correlation with an R^2 of 0.69. If we convert these same values into monthly means, the R^2 is 0.84 and there is no evidence for bias between the two datasets. However, these monthly means are based on only 1-8 samples per month. If instead we calculate the monthly means for the entire surface UV dataset and compare with the monthly means from the ozonesonde data, the data do not compare as well.

To be consistent with the sonde data, it makes the most sense to use only daytime data for this comparison, since the ozonesondes are only launched during daytime. We found the comparison worse if we compared the sonde data with the 24 hour surface monitoring data. Comparing daytime monthly means from Rocky Flats and Boulder surface monitoring data with the ozonesonde data gives R^2 values of 0.65 and 0.60, respectively. On the other hand, if we compare the daytime monthly means from the two surface monitoring sites, we get an R^2 of 0.95. This indicates that spatial variability plays a minor role in this analysis. The ozonesonde launch site is between the South Boulder and Rocky Flats surface monitoring locations. So the larger variations between the ozonesonde and surface monitoring monthly means are due to under-sampling of the parent ozone distribution and/or a larger inherent variability in the ozone measurement technique. The UV method has a precision of about 1 ppbv, compared to the precision of the ECC sonde of about 4 ppbv.

Using the methods from Tiao et al. (1990) and Weatherhead et al. (1998, 2000) we can estimate how the larger variability in ozonesonde monthly means impacts trend detection. The model is based on analysis of the deseasonalized monthly mean (DSMM) O_3 mixing ratio. The essential difference between the two datasets is that the DSMM values for the ozonesonde data have a 1 sigma value of 18.2 %, as compared to the 1 sigma values for the surface data of 9.4 and 14.0% for the two sites considered. This larger variability results in a ~50% increase in the time to detect comparable trends, compared with the continuous surface monitoring data.

6. Evaluation of the role of fire on O_3 at 9 rural sites in the western U.S.

It is well known that fires play an important role in regional air quality. To evaluate the role that fires play on air quality in the western U.S. we have used a database of fires developed by Anthony Westerling (Westerling et al., 2003). A very recent evaluation of these data suggest that large fires in the western U.S. have increased significantly over the past several decades, in response to warmer and dryer climatic conditions (Westerling et al., 2006). This suggests that fires will play an increasingly important role in air quality in the U.S., especially for the western U.S. Our analysis focused on O_3 and PM impacts. In this section we describe the work on O_3 and in the next section, results for PM are presented.

We evaluated the role of fires on daytime O_3 at 9 sites with long-term data in the western U.S. These sites are the same as those described previously for the trends analysis (see Table 1.1 and Figure 1.1). The fire database (provided by A.Westerling) was developed based on county, state and federal reports, as archived at the National Interagency Fire Center (Missoula, MT). The dataset was provided as an ASCII file consisting of monthly area burned on a 1^o x 1^o grid for the western U.S. Fires were assigned to the month of their start date, which did not account for fires that burned over the month divisions. In other words, a fire that burned from July 29-August 5 would be assigned only to the month of July.

Figure 6.1 shows daytime summer mean O_3 mixing ratio at the 9 sites, along with the area burned for each summer. For this figure, we have used the area burned for the entire western U.S.region (36^o-49^o N, 105^o-125^o W). Figure 6.1 shows two important features:

1) There are significant interannual variations in O_3 at these 9 sites and these variations appear to be linked at most sites.
2) There appears to be a correlation between the area burned for the entire western U.S. with summer mean O_3 at most sites. For example, the large fire years of 1996 and 2000 clearly show up as years with enhanced summertime O_3 at nearly all sites. O_3 concentrations in the summer of 2004 were clearly lower at all sites, as was the area burned.

These results are discussed in greater detail below.

Figure 6.1: Daytime summer mean O_3 mixing ratio at 9 sites in the western U.S. (ppbv, left axis) and summer area burned for 36°-49° N and 105-125° W. The area burned (right axis) is given in 10^6 acres. Summer is defined as the months of June, July and August. For this time period, the mean summer area burned is 1.68 million acres.

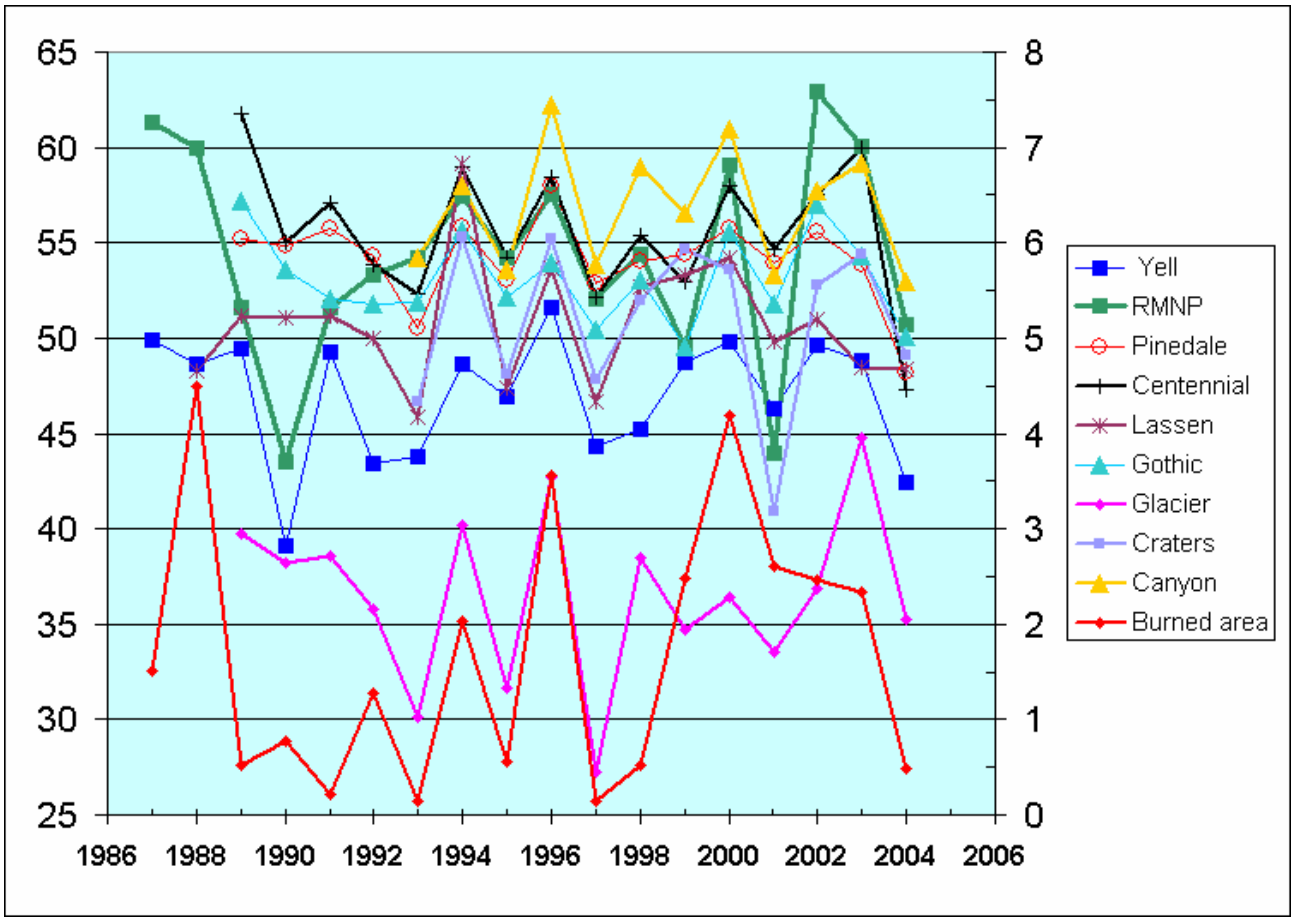

Next, we calculated a correlation matrix to explore the relationship between sites and area burned. These results are shown in Table 6.1, below.

Table 6.1: Correlation matrix for summer (June-August) daytime O_3 between sites and with Area burned in the western U.S (36^o-49^o N and 105^o-125^o W). The correlation coefficient (R), the P-value, and the number of data points are given for each relationship, where each data point represents the mean value for one summer. Correlations significant at P<0.01 are marked with (**) and correlations significant at P<0.05 are marked with (*).

		Rocky Mtn.	Pinedale	Centennial	Lassen	Gothic	Glacier	Craters	Canyonld	Burn area
Yellowstone	R	.718(**)	.769(**)	.718(**)	.618(**)	.704(**)	.422	.704(*)	.852(**)	.528(*)
	Sig. (2-tailed)	.001	.001	.002	.008	.002	.104	.011	.000	.024
	N	18	16	16	17	16	16	12	12	18
Rocky Mtn.	R	1	.553(*)	.577(*)	.393	.756(**)	.359	.738(**)	.703(*)	.453
	Sig. (2-tailed)		.026	.019	.118	.001	.172	.006	.011	.059
	N	18	16	16	17	16	16	12	12	18
Pinedale	R	.553(*)	1	.812(**)	.707(**)	.685(**)	.526(*)	.558	.779(**)	.836(**)
	Sig. (2-tailed)	.026		.000	.002	.003	.036	.059	.003	.000
	N	16	16	16	16	16	16	12	12	16
Centennial	R	.577(*)	.812(**)	1	.529(*)	.812(**)	.680(**)	.548	.756(**)	.647(**)
	Sig. (2-tailed)	.019	.000		.035	.000	.004	.065	.004	.007
	N	16	16	16	16	16	16	12	12	16
Lassen	R	.393	.707(**)	.529(*)	1	.590(*)	.551(*)	.672(*)	.663(*)	.383
	Sig. (2-tailed)	.118	.002	.035		.016	.027	.017	.019	.130
	N	17	16	16	17	16	16	12	12	17
Gothic	R	.756(**)	.685(**)	.812(**)	.590(*)	1	.541(*)	.569	.771(**)	.620(*)
	Sig. (2-tailed)	.001	.003	.000	.016		.031	.054	.003	.010
	N	16	16	16	16	16	16	12	12	16
Glacier	R	.359	.526(*)	.680(**)	.551(*)	.541(*)	1	.753(**)	.821(**)	.459
	Sig. (2-tailed)	.172	.036	.004	.027	.031		.005	.001	.074
	N	16	16	16	16	16	16	12	12	16
Craters	R	.738(**)	.558	.548	.672(*)	.569	.753(**)	1	.819(**)	.504
	Sig. (2-tailed)	.006	.059	.065	.017	.054	.005		.001	.094
	N	12	12	12	12	12	12	12	12	12
Canyonlnd	R	.703(*)	.779(**)	.756(**)	.663(*)	.771(**)	.821(**)	.819(**)	1	.729(**)
	Sig. (2-tailed)	.011	.003	.004	.019	.003	.001	.001		.007
	N	12	12	12	12	12	12	12	12	12
Burn area	R	.453	.836(**)	.647(**)	.383	.620(*)	.459	.504	.729(**)	1
	Sig. (2-tailed)	.059	.000	.007	.130	.010	.074	.094	.007	
	N	18	16	16	17	16	16	12	12	18

As a test of this method, we also calculated correlation coefficients for summer mean O_3 at Denali National Park in Alaska with area burned in the western U.S. As expected, the correlation was not significant (R^2 of 0.04).

The results in Table 6.1 demonstrate that the interannual variations in O_3 at these sites are highly correlated and that area burned is an important variable that helps explain this relationship. The average slope from these 9 sites is 1.68×10^{-6} ppbv/acre burned, with a range of 1.04-2.03 $\times 10^{-6}$ and a standard deviation of 0.31×10^{-6} ppbv/acre burned. So for a large fire year, such as 2000 with 4.19 million acres burned, we can expect the mean summer O_3 concentration in the western U.S. to be enhanced by 7 ppbv. This is a significant increase and will likely play an important role in the frequency of days with 8-hour averages greater than 0.08 ppmv. Note that 1999-2003 were all above average years for fires in the western U.S., and O_3 was generally enhanced at all 9 sites (see Figure 6.1).

We also evaluated this correlation using the monthly O_3 and area burned data. Table 6.2, below, has these results.

Table 6.2: Correlation matrix for monthly (June-August) daytime O_3 between sites and with Area burned in the western U.S. (36^o-49^o N and 105^o-125^o W). The correlation coefficient (R), the P-value and the number of data points are given for each relationship, where each data point represents the mean value for one month. Correlations significant at P<0.01 are marked with (**) and correlations significant at P<0.05 are marked with (*).

		Rocky Mtn	PInedale	Centennial	Lassen	Gothic	Glacier	Crater	CanyonInd	Burn area
Yellowstone	R	.600(**)	.706(**)	.670(**)	.445(**)	.571(**)	.403(**)	.707(**)	.742(**)	.282(*)
	Sig. (2-tailed)	.000	.000	.000	.001	.000	.004	.000	.000	.039
	N	53	46	46	51	47	48	36	37	54
Rocky Mtn.	R	1	.528(**)	.646(**)	.339(*)	.639(**)	.304(*)	.673(**)	.634(**)	.383(**)
	Sig. (2-tailed)		.000	.000	.015	.000	.036	.000	.000	.005
	N	53	46	46	51	47	48	36	37	53
Pinedale	R	.528(**)	1	.780(**)	.582(**)	.550(**)	.486(**)	.548(**)	.670(**)	.540(**)
	Sig. (2-tailed)	.000		.000	.000	.000	.001	.001	.000	.000
	N	46	46	44	46	45	46	34	35	46
Centennial	R	.646(**)	.780(**)	1	.447(**)	.735(**)	.614(**)	.570(**)	.744(**)	.498(**)
	Sig. (2-tailed)	.000	.000		.002	.000	.000	.000	.000	.000
	N	46	44	46	46	46	46	36	37	46
Lassen	R	.339(*)	.582(**)	.447(**)	1	.241	.426(**)	.619(**)	.509(**)	.351(*)
	Sig. (2-tailed)	.015	.000	.002		.103	.003	.000	.001	.012
	N	51	46	46	51	47	48	36	37	51
Gothic	R	.639(**)	.550(**)	.735(**)	.241	1	.396(**)	.393(*)	.746(**)	.215
	Sig. (2-tailed)	.000	.000	.000	.103		.006	.018	.000	.147
	N	47	45	46	47	47	47	36	37	47
Glacier	R	.304(*)	.486(**)	.614(**)	.426(**)	.396(**)	1	.689(**)	.663(**)	.335(*)
	Sig. (2-tailed)	.036	.001	.000	.003	.006		.000	.000	.020
	N	48	46	46	48	47	48	36	37	48
Crater	R	.673(**)	.548(**)	.570(**)	.619(**)	.393(*)	.689(**)	1	.717(**)	.427(**)
	Sig. (2-tailed)	.000	.001	.000	.000	.018	.000		.000	.009
	N	36	34	36	36	36	36	36	36	36
CanyonInd	R	.634(**)	.670(**)	.744(**)	.509(**)	.746(**)	.663(**)	.717(**)	1	.447(**)
	Sig. (2-tailed)	.000	.000	.000	.001	.000	.000	.000		.006
	N	37	35	37	37	37	37	36	37	37
Burn area	R	.383(**)	.540(**)	.498(**)	.351(*)	.215	.335(*)	.427(**)	.447(**)	1
	Sig. (2-tailed)	.005	.000	.000	.012	.147	.020	.009	.006	
	N	53	46	46	51	47	48	36	37	54

In general, the results using monthly data are similar to the results using seasonal means, but the correlation with area burned is lower for every site. While we might expect an improvement when using the monthly data, this was not seen, probably due to the limitations on the area burned dataset. Recall that fires are assigned to the start month and so the monthly area burned may not accurately reflect the true area burned. On the other hand, we expect that the summer area burned should accurately reflect variations between one year and the next.

Of the locations listed in Table 6.2, 7 sites have data going back to at least 1989. Averaging the data from these 7 sites (excludes Craters of the Moon and Canyonlands) we get a reasonable correlation between O_3 and area burned. Figure 6.2 shows a time series and Figure 6.3 a scatterplot.

Figure 6.2: Time series of seasonal mean O_3 averaged from 7 sites (circles) and area burned in the western U.S. (squares).

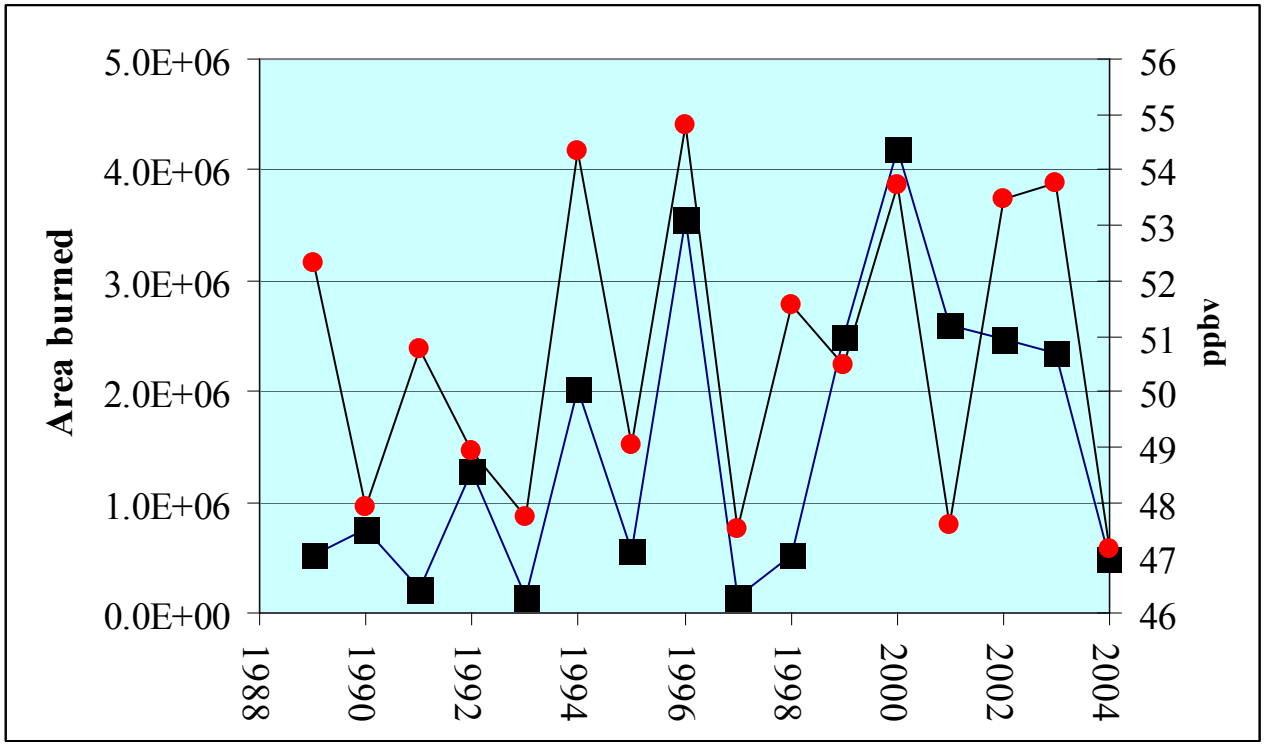

Figure 6.3: Scatterplot of seasonal mean O_3 average at 7 sites vs area burned in the western U.S.

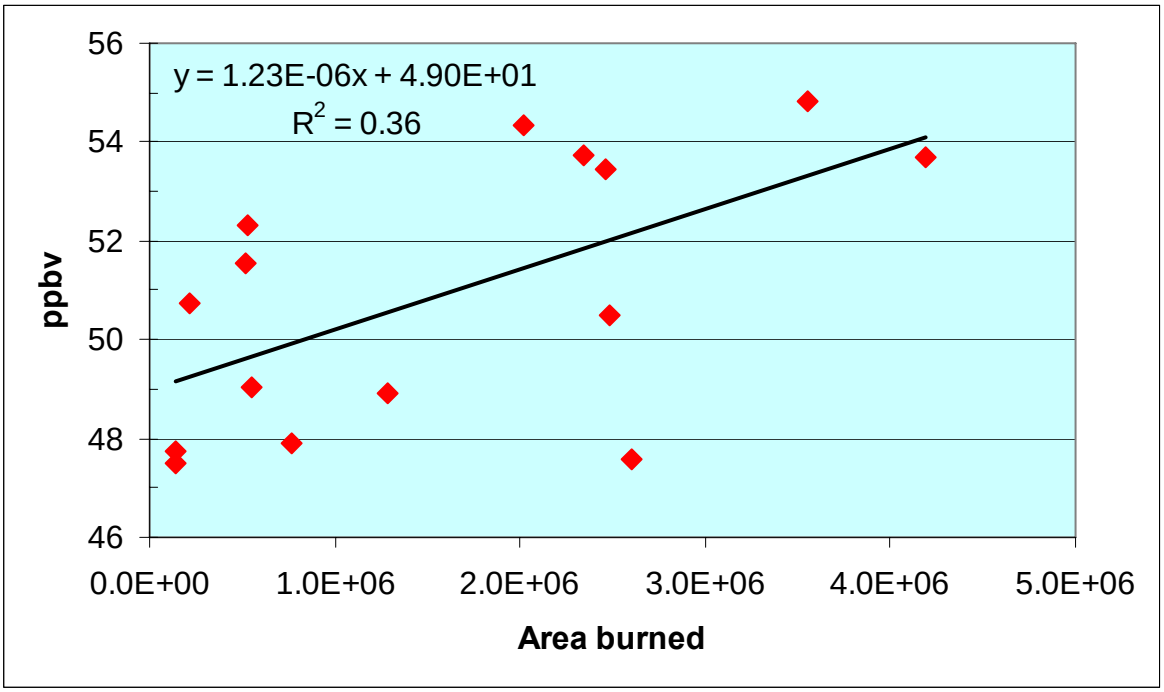

Next, we will examine the relationship between area burned in the region of each monitoring site, rather then for the entire western U.S. For this, we have used the summer mean O_3 concentrations and summer area burned values. The regional boundaries and summer area burned values are given in Table 6.3 and a map showing the approximate regions is shown in Figure 6.2.

Table 6.3: Summer (June, July and August) area burned for various regions in the U.S.

Year	Western US area burned (acres)	Region 1: Western Rocky Mtn area burned (acres)	Region 2: Colorado area burned (acres)	Region 3: N.California area burned (acres)
Lat./long.	**36^o-49^o N 105^o-125^o W**	**37^o-47^oN 110^o-117^o W**	**37^o-42^oN 105^o-110^oW**	**37^o-42^oN 119^o -125^o W**
1987	1.51E+06	2.92E+05	2.90E+04	7.29E+05
1988	4.50E+06	3.16E+06	4.65E+04	3.18E+04
1989	5.29E+05	2.91E+05	4.81E+04	2.33E+04
1990	7.65E+05	1.96E+05	1.62E+04	2.93E+05
1991	2.13E+05	1.33E+05	9.86E+02	1.99E+03
1992	1.28E+06	8.47E+05	2.93E+03	2.15E+05
1993	1.45E+05	5.26E+04	3.29E+04	1.44E+03
1994	2.02E+06	9.91E+05	6.50E+04	1.46E+05
1995	5.55E+05	4.10E+05	1.63E+04	9.07E+03
1996	3.55E+06	1.60E+06	4.55E+04	3.27E+05
1997	1.42E+05	5.82E+04	7.00E+03	1.24E+04
1998	5.20E+05	2.17E+05	9.65E+03	3.39E+04
1999	2.49E+06	1.12E+06	2.25E+04	4.08E+05
2000	4.19E+06	2.51E+06	1.56E+05	1.29E+05
2001	2.60E+06	6.27E+05	1.69E+04	2.40E+05
2002	2.47E+06	1.67E+05	6.17E+05	1.09E+05
2003	2.34E+06	4.09E+05	5.94E+04	4.58E+04
2004	4.87E+05	5.39E+04	3.56E+04	5.69E+04
Average	1.68E+06	7.30E+05	6.82E+04	1.56E+05

Figure 6.4: Location of O_3 monitoring sites and the approximate boundaries used to define various regions for analysis of area burned. Region 1, 2, and 3 are shown by the blue, red and purple boxes, respectively.

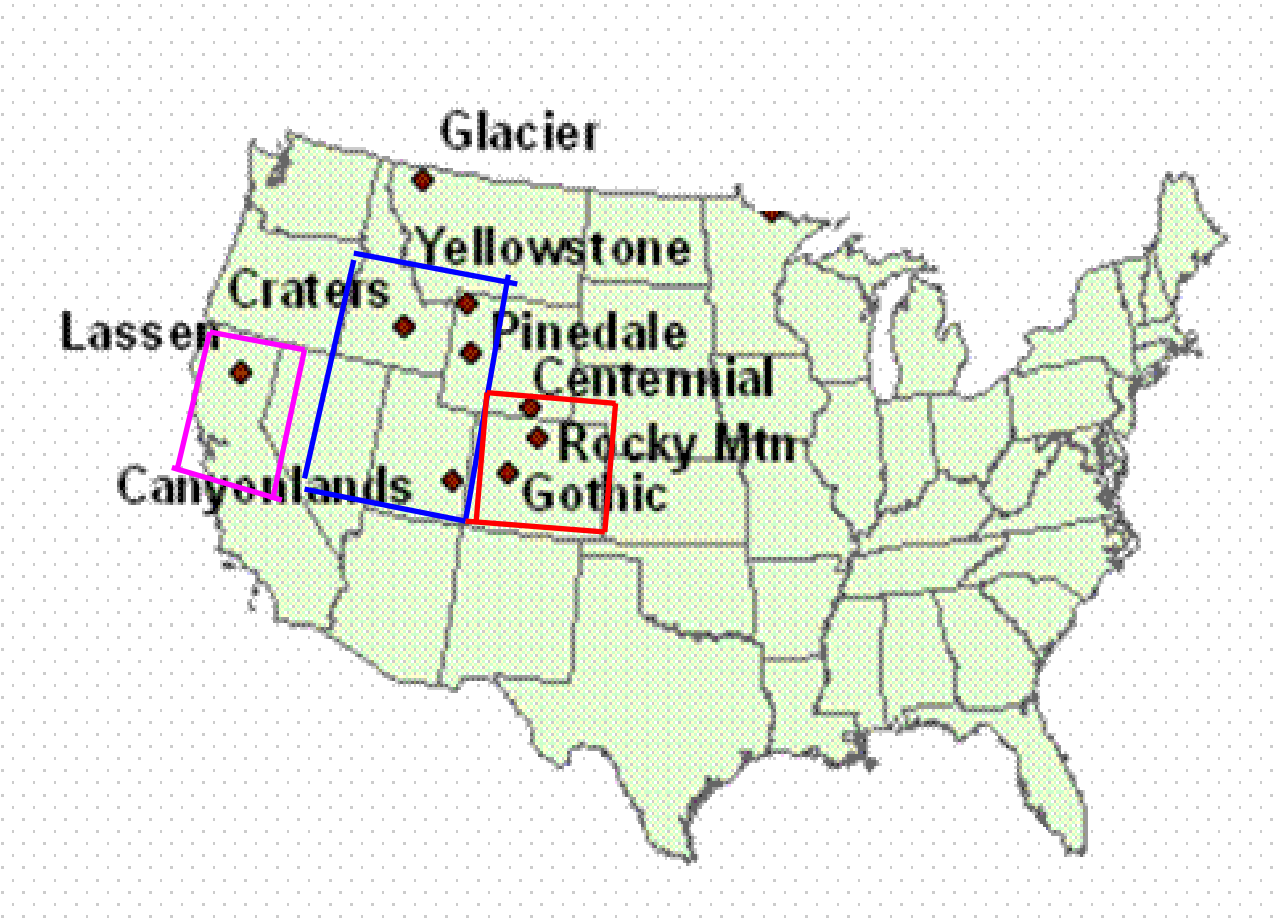

However, the regional area burned datasets are not normally distributed. There is a significant skew, with a few years having very high values. For this reason, it is necessary to consider the relationship between O_3 and the log of the regional area burned. After taking the natural log of the regional area burned datasets, these are approximately Gaussian. The correlation matrix for these results is shown in Table 6.4 below.

Table 6.4: Correlation matrix between summer mean O_3 and regional area burned for 3 regions in the Western U.S. Values marked with * are significant at P<0.05 and values marked with ** are significant at P<0.01.

		Ln Burned area 1: Western Rockies	Ln Burned area 2: Colorado	Ln Burned area 3: N.California
Yellowstone	R	.332	.497(*)	.159
	Sig. (2-tailed)	.178	.036	.530
	N	18	18	18
Rocky Mtn.	R	.190	.628(**)	.068
	Sig. (2-tailed)	.451	.005	.790
	N	18	18	18
Pinedale	R	.650(**)	.434	.538(*)
	Sig. (2-tailed)	.006	.093	.032
	N	16	16	16
Centennial	R	.524(*)	.534(*)	.255
	Sig. (2-tailed)	.037	.033	.340
	N	16	16	16
Lassen	R	.347	.391	.610(**)
	Sig. (2-tailed)	.172	.121	.009
	N	17	17	17
Gothic	R	.286	.831(**)	.314
	Sig. (2-tailed)	.283	.000	.236
	N	16	16	16
Glacier	R	.430	.292	.392
	Sig. (2-tailed)	.096	.273	.134
	N	16	16	16
Crater	R	.404	.533	.528
	Sig. (2-tailed)	.193	.074	.078
	N	12	12	12
Canyonlands	R	.507	.549	.623(*)
	Sig. (2-tailed)	.093	.065	.031
	N	12	12	12

Some of the results in Table 6.4 are as we would expect. For example for Rocky Mtn, Pinedale, Lassen and Gothic, the best O_3-burned area correlation is found when using the area burned from the same region as the site location. However, for some sites a more surprising results is found. For example, Yellowstone O_3 correlates better with area burned in Colorado, then with area burned for the western Rockies. This largely reflects the fact that despite huge 1988 Yellowstone fires (Region 1), the summer mean O_3 at Yellowstone was not significantly enhanced in that year (see Figure 6.1). In contrast, PM2.5 data from Yellowstone N.P in the summer of 1988 was significantly enhanced due to the fires. Possibly, the very close proximity of the fires to the monitoring site resulted in significant NOx titration and prevented significant O_3 buildup. Transport of smoke from one region to another is also clearly indicated by the results in Table 6.4. For example, Pinedale and Canyonlands show significant correlation with area burned in N. California and most sites show some positive correlation with the area burned in other regions.

We have evaluated O_3 and area burned data for 1987-2004. During this period, there has been an increase in fire activity in the western U.S. For example, between 1999-2003, the summer burned areas averaged 72% greater than the average for 1987-2004 time period. Comparing the later 9 years of this data record (1996-2004), with the first 9 years, (1987-1995) we find the area burned increased by 63%. Comparing the data back to 1950, Westerling et al. (2006) has recently reported that fires in the western U.S. are increasing as a result of climate change. Given that O_3 is clearly correlated with area burned, we believe the increasing frequency of large fires is a likely contributor to the O_3 trend that we reported in section 2 of this report. However, given that fires will only be significant during late spring-fall, and the ozone trends appear to be present in all seasons, increasing fires must not be the only cause for the O_3 trends.

7. Evaluation of the role of fire on PM2.5 at 29 rural IMPROVE sites in the western U.S.

Using the same fire database as mentioned in the earlier sections, we can examine the relationship between area burned and PM2.5 concentrations in the western U.S. For this analysis we used PM2.5 data from 28 IMPROVE sites in the western U.S. Again as a test of the method, we included data from Denali N.P. in Alaska. It should be kept in mind that since IMPROVE samples are only taken 2 days per week, PM from some fires will be missed at all sites.

A list of the sites used in this analysis is given in Table 7.1. A map showing these sites, along with the regional boundaries used for area burned (same as in section 6) is shown in Figure 7.1. In this section, we provide a selection of some of the key results. The complete results are available as an Excel data file from D.Jaffe.

Figure 7.1: IMPROVE sites used in this analysis. Sites are identified by elevation. Also shown are the boundaries used for burned area definitions.

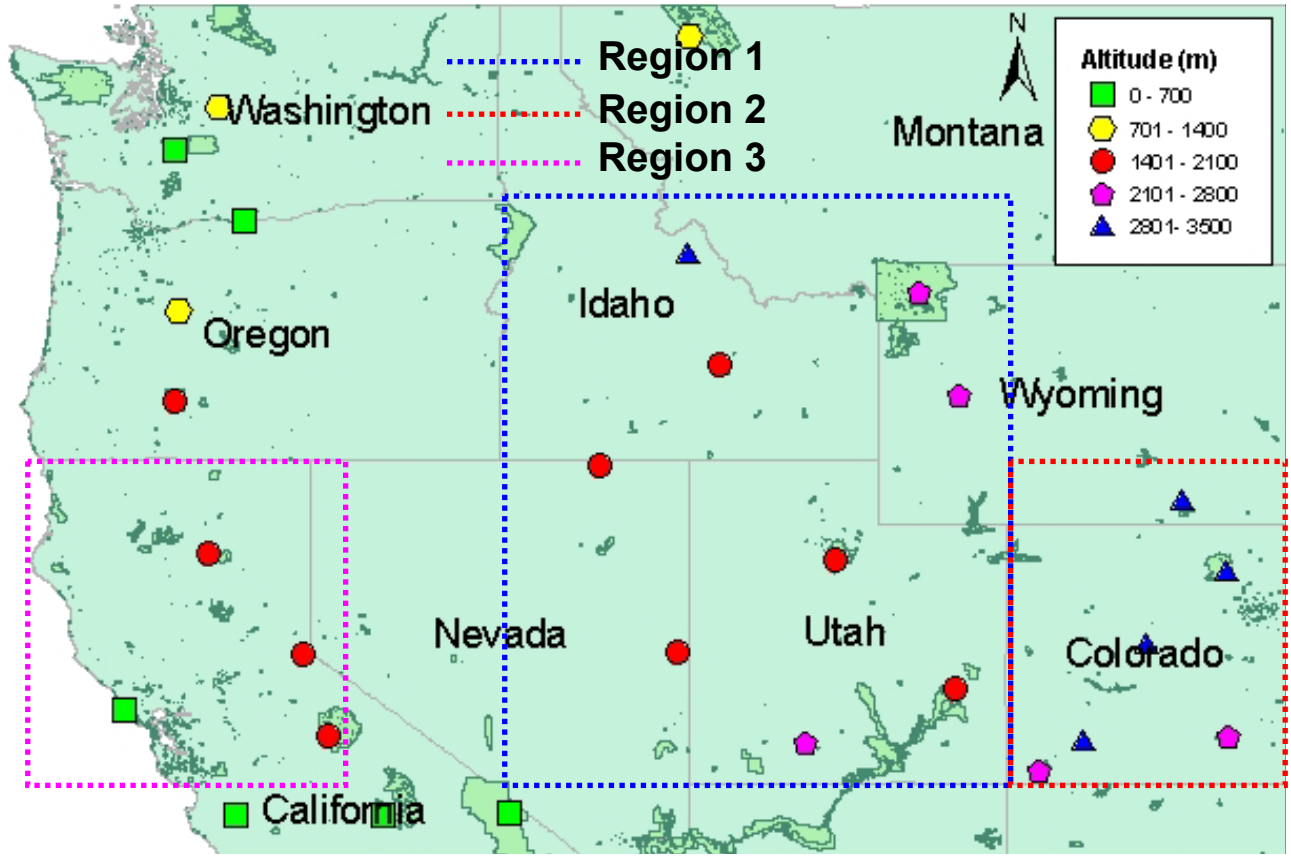

Table 7.1: IMPROVE sites used in this analysis.

Site name	Site code	State	Elevation (meters)	Lat. (^oN)	Long. (^oW)	Start date
Bliss State Park (TRPA)	BLIS	CA	2116	39.0	-120.1	11/1990
Bryce Canyon National Park	BRCA	UT	2477	37.6	-112.2	3/1988
Brooklyn Lake	BRLA	WY	3196	41.4	-106.2	7/1993
Bridger Wilderness	BRID	WY	2607	43.0	-109.8	3/1988
Canyonlands National Park	CANY	UT	1799	38.5	-109.8	3/1988
Columbia River Gorge	CORI	WA	201	45.7	-121.0	6/1993
Crater Lake National Park	CRLA	OR	1963	42.9	-122.1	3/1988
Craters of the Moon NM(US DOE)	CRMO	ID	1817	43.5	-113.6	5/1992
Denali National Park	DENA	AK	658	63.7	-149.0	3/1988
Death Valley Monument	DEVA	CA	125	36.5	-116.8	10/1993
Glacier National Park	GLAC	MT	979	48.5	-114.0	3/1988
Great Basin National Park	GRBA	NV	2068	39.0	-114.2	5/1992
Great Sand Dunes National Monument	GRSA	CO	2504	37.7	-105.5	5/1988
Jarbidge Wilderness	JARB	NV	1882	41.9	-115.4	3/1988
Lassen Volcanic National Park	LAVO	CA	1755	40.5	-121.6	3/1988
Lone Peak Wilderness	LOPE	UT	1768	40.4	-111.7	12//1993
Mesa Verde National Park	MEVE	CO	2177	37.2	-108.5	3/1988
Mount Rainier National Park	MORA	WA	427	46.8	-122.1	3/1988
Pinnacles National Monument	PINN	CA	317	36.5	-121.2	3/1988
Point Reyes National Seashore	PORE	CA	85	38.1	-122.9	3/1988
Rocky Mountain National Park	ROMO	CO	2755	40.3	-105.5	9//1990
Salmon National Forest	SALM	ID	2788	45.2	-114.0	12/1993
Sequoia National Park	SEQU	CA	535	36.5	-118.8	3/1992
Snoqualmie Pass; Snoqualmie N.F	SNPA	WA	1160	47.4	-121.4	7/1993
Three Sisters	THIS	OR	885	44.3	-122.0	7/1993

Wilderness						
Weminuche Wilderness	WEMI	CO	2765	37.7	-107.8	3/1988
White River National Forest	WHRI	CO	3418	39.2	-106.8	7/1993
Yosemite National Park	YOSE	CA	1615	37.7	-119.7	3/1988
Yellowstone National park	YELL	WY	2425	44.6	-110.4	3/1988

As with O_3, we examined the relationship between sites of seasonal mean PM2.5 to examine the degree of spatial correlation. We also examined the correlation between PM2.5 and area burned using both seasonal and monthly data, and using area burned for the entire western U.S., as well as by regions. In general, we found that there was no advantage in using monthly correlations, probably due to the limits of the fire dataset, mentioned above. Table 7.2 presents a selection of these results.

Table 7.2: Correlation of summer (June, July, August) mean PM2.5 and Western U.S. burned area for 29 IMPROVE sites.

		DENA	ROMO	GRBA	W.US Burned area (acres)
BLIS	R	-0.11	0.40	0.41	0.01
	Sig. (2-tailed)	0.72	0.18	0.19	0.97
	N	13.00	13.00	12.00	13.00
BRCA	R	0.21	0.70	0.72	0.29
	Sig. (2-tailed)	0.42	0.00	0.01	0.26
	N	17.00	17.00	13.00	17.00
BRLA	R	-0.33	0.94	0.79	0.47
	Sig. (2-tailed)	0.35	0.00	0.01	0.18
	N	10.00	10.00	10.00	10.00
BRID	R	-0.05	0.71	0.77	0.64
	Sig. (2-tailed)	0.84	0.00	0.00	0.01
	N	17.00	17.00	13.00	17.00
CANY	R	-0.06	0.87	0.74	0.10
	Sig. (2-tailed)	0.81	0.00	0.00	0.70
	N	17.00	17.00	13.00	17.00
CORI	R	-0.43	0.26	0.47	0.29
	Sig. (2-tailed)	0.19	0.44	0.15	0.38
	N	11.00	11.00	11.00	11.00
CRLA	R	0.06	0.64	0.65	0.19
	Sig. (2-tailed)	0.84	0.01	0.02	0.48
	N	16.00	16.00	12.00	16.00
CRMO	R	0.01	0.58	0.67	0.70
	Sig. (2-tailed)	0.96	0.04	0.01	0.01
	N	13.00	13.00	13.00	13.00

DENA	R		-0.04	-0.13	-0.20
	Sig. (2-tailed)		0.87	0.68	0.44
	N		17.00	13.00	17.00
DEVA	R	-0.22	0.85	0.76	0.36
	Sig. (2-tailed)	0.51	0.00	0.01	0.28
	N	11.00	11.00	11.00	11.00
GLAC	R	0.10	0.13	0.00	0.54
	Sig. (2-tailed)	0.69	0.61	1.00	0.02
	N	17.00	17.00	13.00	17.00
GRBA	R	-0.13	0.68		0.53
	Sig. (2-tailed)	0.68	0.01		0.06
	N	13.00	13.00		13.00
GRSA	R	-0.08	0.84	0.51	0.08
	Sig. (2-tailed)	0.77	0.00	0.07	0.75
	N	17.00	17.00	13.00	17.00
JARB	R	0.23	0.49	0.52	0.51
	Sig. (2-tailed)	0.37	0.05	0.07	0.04
	N	17.00	17.00	13.00	17.00
LAVO	R	-0.36	0.53	0.55	0.34
	Sig. (2-tailed)	0.16	0.03	0.05	0.19
	N	17.00	17.00	13.00	17.00
LOPE	R	-0.17	0.34	0.89	0.66
	Sig. (2-tailed)	0.69	0.41	0.00	0.08
	N	8.00	8.00	8.00	8.00
MEVE	R	0.00	0.63	0.67	0.25
	Sig. (2-tailed)	0.99	0.01	0.01	0.34
	N	17.00	17.00	13.00	17.00
MORA	R	-0.08	0.07	0.44	-0.10
	Sig. (2-tailed)	0.77	0.81	0.13	0.71
	N	16.00	16.00	13.00	16.00
PINN	R	0.34	0.38	0.50	-0.15
	Sig. (2-tailed)	0.18	0.13	0.08	0.56
	N	17.00	17.00	13.00	17.00
PORE	R	-0.33	0.48	0.57	0.13
	Sig. (2-tailed)	0.19	0.05	0.04	0.62
	N	17.00	17.00	13.00	17.00
ROMO	R	-0.04		0.68	0.27
	Sig. (2-tailed)	0.87		0.01	0.30
	N	17.00		13.00	17.00
SALM	R	0.30	0.37	0.04	0.71
	Sig. (2-tailed)	0.52	0.41	0.94	0.08
	N	7.00	7.00	7.00	7.00
SEQU	R	0.06	0.35	0.60	0.17
	Sig. (2-tailed)	0.85	0.24	0.03	0.59
	N	13.00	13.00	13.00	13.00
SNPA	R	0.24	0.09	0.30	-0.20
	Sig. (2-tailed)	0.45	0.78	0.35	0.52
	N	12.00	12.00	12.00	12.00
THSI	R	-0.01	0.18	0.42	-0.19
	Sig. (2-tailed)	0.96	0.59	0.17	0.56
	N	12.00	12.00	12.00	12.00
WEMI	R	0.08	0.77	0.73	0.05

	Sig. (2-tailed)	0.76	0.00	0.00	0.84
	N	17.00	17.00	13.00	17.00
WHRI	R	-0.09	0.93	0.79	0.47
	Sig. (2-tailed)	0.78	0.00	0.00	0.13
	N	12.00	12.00	12.00	12.00
YOSE	R	-0.29	0.28	0.74	0.50
	Sig. (2-tailed)	0.26	0.27	0.00	0.04
	N	17.00	17.00	13.00	17.00
YELL	R	-0.31	0.18	0.58	0.69
	Sig. (2-tailed)	0.24	0.51	0.05	0.00
	N	16.00	16.00	12.00	16.00

These data show that there is a significant spatial correlation in seasonal mean PM2.5 concentrations. For example, Rocky Mtn is significantly correlated with 14 of the 29 sites and Great Basin (GRBA) is correlated with 15. In contrast, Denali (DENA) is not significantly correlated with any of the continental U.S. sites. We also correlated PM2.5 for each site with area burned for the entire western U.S and find that only 6 sites are individually correlated.

By averaging over larger regions we can improve these relationships. Figures 7.2 and 7.3 shows the relationship between average PM2.5 and Western U.S. fires

Figure 7.2: Time series of summer mean PM2.5 averaged over 4,20 and 29 sites in the western U.S.

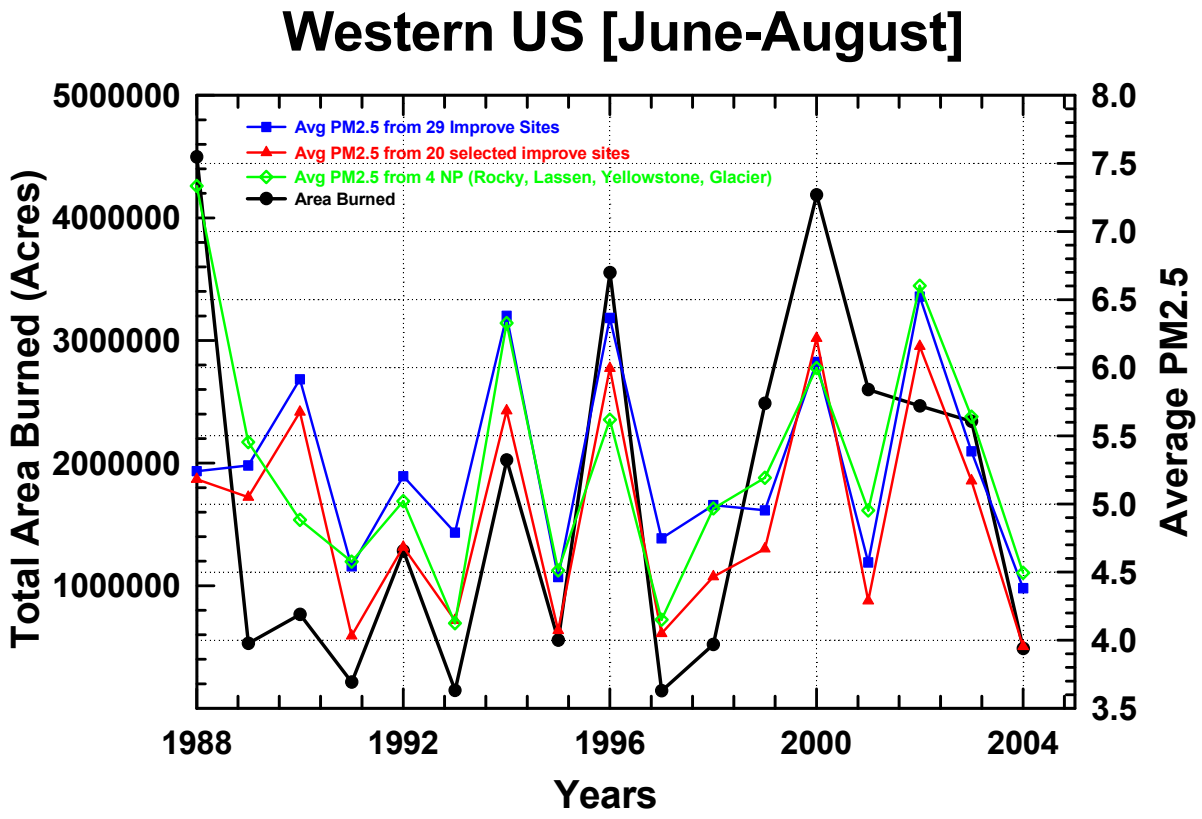

Figure 7.3: Scatterplot of summer mean PM2.5 averaged over 29,20 and 4 sites, along with area burned in the western U.S. for the years 1988-2004. The R^2 for each correlation is 0.28, 0.44 and 0.64, respectively for 29, 20 and 4 sites.

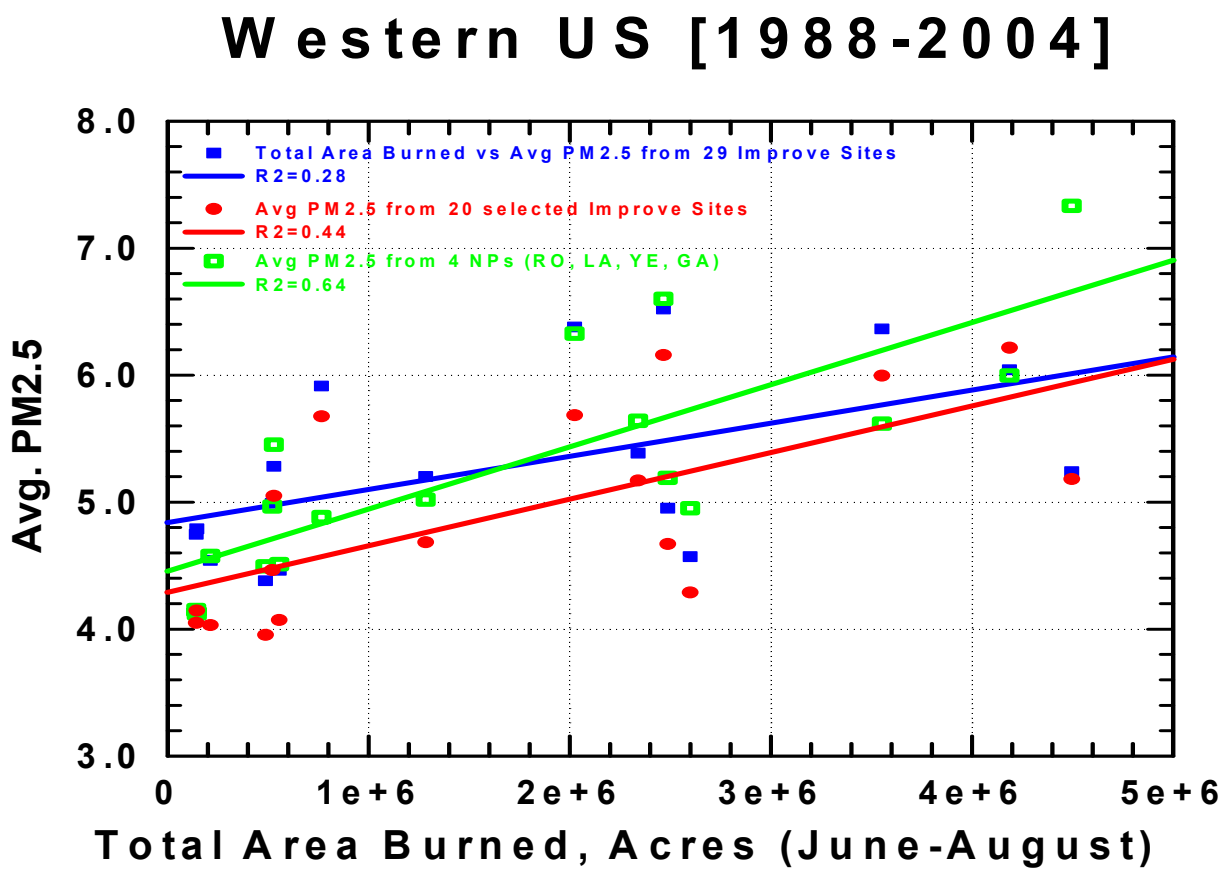

The relationship between area burned (acres) and PM2.5 (20 site average) is:

PM 2.5 = 3.67E-07 * acres + 4.29

R^2 = 0.44

This relationship is slightly different if we use only 4 sites instead (ROMO, LAVO, YELL, GLAC)

PM 2.5 = 4.90E-07 * acres + 4.46

R^2 = 0.64

Using these relationships, we can estimate the contribution that fires make to PM2.5 in the western U.S. during an average fire year. During this time period (1988-2004) the mean annual

area burned was 1.69 E6 acres. Using the relationships above, this corresponds to a PM2.5 enhancement of 0.58-0.78 $\mu g/m^3$.

To analyze the PM2.5 data with area burned by region, we used the same burned regions as was used in Section 6. For PM2.5 data, we averaged data from several sites in the region that have similar length data records. The results of the correlations are shown in Table 7.3 and Figure 7.2 shows a time series of Region 1 PM2.5 with area burned in Regions 1 and 2.

Table 7.3: Correlation of summer mean PM2.5 and area burned for 3 regions, as shown in Figure 7.1. Correlations significant at P<0.01 are marked with (**) and correlations significant at P<0.05 are marked with (*).

		LN Burned area Region 1 (Rocky Mtns)	LN Burned area Region 2 (Colorado)	LN Burned area Region 3 (N.California)
Region 1 PM2.5: BRCA, BRID, CANY, YELL, JARB	**R**	.580(*)	.521(*)	.547(*)
	Sig. (2-tailed)	.015	.032	.023
	N	17	17	17
Region 2 PM2.5: GRSA, MEVE, ROMO, WEMI	**R**	.000	.593(*)	.294
	Sig. (2-tailed)	1.000	.012	.252
	N	17	17	17
Region 3 PM2.5: LAVO, YOSE	**R**	.351	.591(*)	.464
	Sig. (2-tailed)	.168	.012	.061
	N	17	17	17

Figure 7.4: Time series of summer average PM2.5 for region 1, with natural log of area burned in regions 1 and 2.

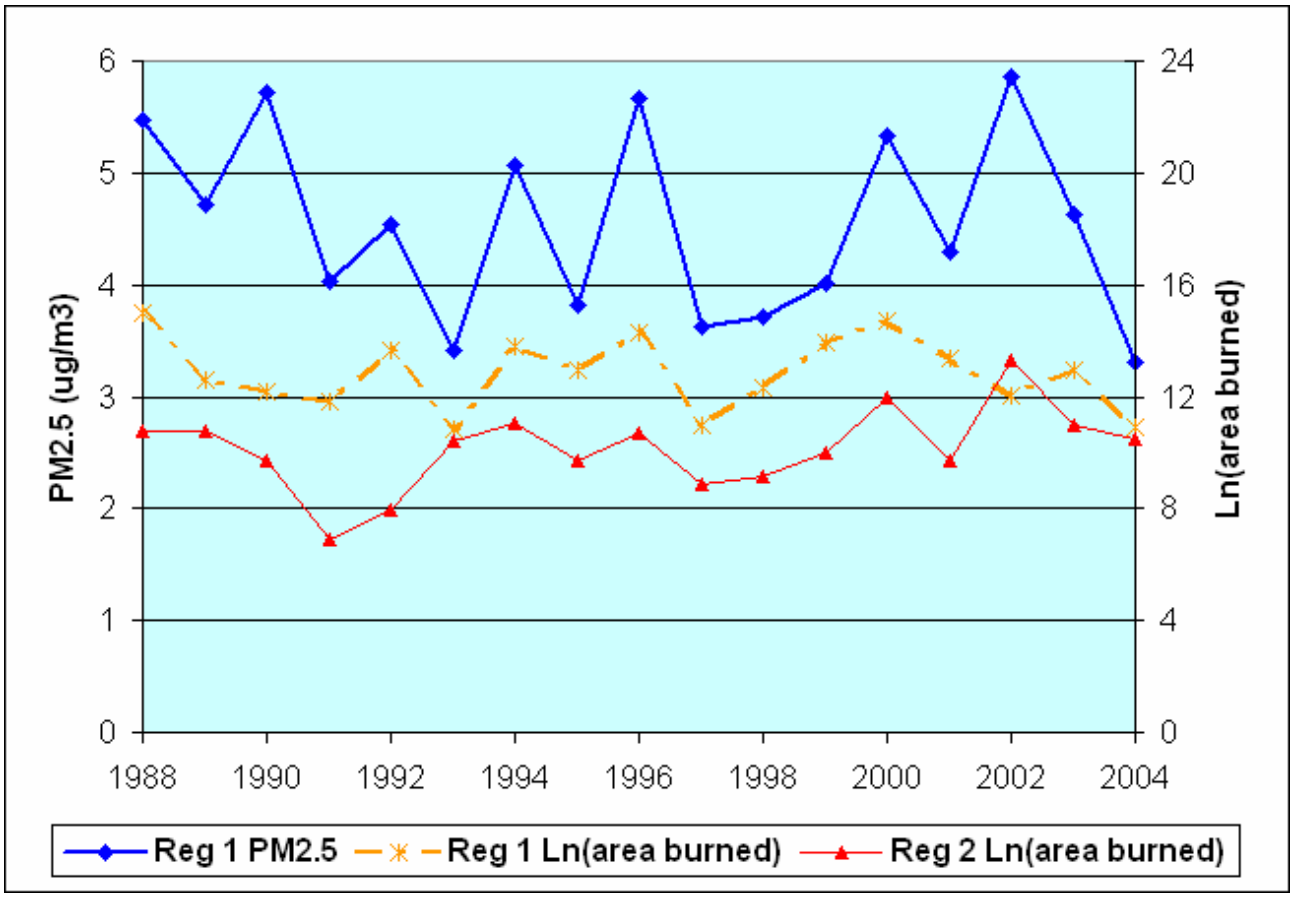

For regions 1 and 2, there is a good correlation between summer mean PM2.5 and area burned in the same region. PM2.5 in region 1 is also significantly correlated with the area burned in regions 2 and 3, which indicates transport of smoke. This is seen in Figure 7.2. For example in 2002, large fires burned in region 2 (Colorado), and PM at sites in region 1 were likely impacted. The results for region 3 are somewhat puzzling. The most significant correlation for PM2.5 in region 3 was with area burned in region 2 (Colorado). We have no good explanation for this result. The correlation between area burned in region 3 with PM2.5 in region 3 was nearly significant, with a P value of 0.06, however this reflects only 2 sites with similar length data records.

From the significant correlations, we can estimate the contribution of fires to PM2.5 in each regions 1 and 2 using the following:

PM2.5 (region x) = a* Ln(burned area 1) + b* Ln(burned area 2) + c * Ln(burned area 3)

Due to the confusing result for region 3, we will only do this calculation for regions 1 and 2. The best estimate coefficients for the equation above are shown in Table 7.4

Table 7.4: Regression coefficients for the relationship between burned area and PM2.5 in each region.

	a	b	c	R^2	P value
PM2.5 region 1	**0.25**	**0.21**	**0.11**	**0.53**	**0.02**
PM2.5 region 2	**NS**	**0.36**	**NS**	**0.35**	**0.01**

These results imply that for a large fire year in region 1, such as 2000 when 2.5 million acres burned in region 1 alone, the summer mean PM2.5 in that region will be enhanced by 3.7 ug/m3, on average. For a large fire year in region 2, such as 2002 when 0.62 million acres burned in that region, the summer mean PM2.5 in that region will be enhanced by 4.8 ug/m3, on average.

In summary, fires are an important contributor to PM2.5 in the western U.S. We have found a significant correlation between area burned and PM2.5 at many IMPROVE monitoring site in the western U.S. Using a regional analysis, we find that interannual variations in area burned can explain 53% of the variance in seasonal mean PM2.5 concentrations for the western Rocky Mtn area (Region 1) and 35% of the variance in the Colorado area (Region 2).

References

Hess, A., Iyer, H., and Malm, W., Linear trend analysis: A comparison of methods, *Atmos. Environ., 35*, 5211-5222, 2001.

Tiao, G.C., et al., Effects of autocorrelation and temporal sampling schemes on estimates of trend and spatial correlation, *J.Geophys.Res., 95*, 20507-20517, 1990.

Weatherhead, E.C., et al., Factors affecting the detection of trends: Statistical considerations and applications to environmental data, *J. Geophys. Res., 103*, 17,149, 1998.

Weatherhead, E.C., et al., Detecting the recovery of total column ozone, *J.Geophys.Res., 105*, 22201-22210, 2000.

Westerling, A.L., Hidalgo, H.G., Cayan, D.R., and Swetnam, T.W., Warming and Earlier Spring Increases Western U.S. Forest Wildfire Activity, *Science, 313,* 940-943, 2006.

Westerling, A.L., Gershunov, T.J., Brown, D.R., Cayan, D.R., and Dettinger, M.D., Climate and Wildfire in the Western United States, *Bull. Amer Met Soc.,* 595-604, May 2003.